PRIMARY DEVELOPMENT OF A PROPANE AIR COMBUSTOR

PRIMARY DEVELOPMENT OF A
PROPANE AIR COMBUSTOR

by

RICHARD ANDREW FRANCIS BENNETT, B.Sc.

A Thesis
Submitted to the Faculty of Graduate Studies
in Partial Fulfilment of the Requirements
for the Degree
Master of Engineering

McMaster University
April 1967

MASTER OF ENGINEERING (1967)
(Mechanical)

MCMASTER UNIVERSITY
Hamilton, Ontario.

TITLE: Primary Development of a Propane Air Combustor

AUTHOR: Richard Andrew Francis Bennett, B.Sc. (Dunelm)

SUPERVISOR: Dr. J. H. T. Wade

NUMBER OF PAGES: (ix) 113

SCOPE AND CONTENTS: The design, and construction of a combustion chamber was undertaken, and the basic considerations, design steps and calculations are described. The preliminary testing consisted of measurements of flame temperature, flame tube wall temperature, and flame tube exit plane temperature. A comparison was made between the experimental and theoretical flame temperatures. The uniformity of air flow in the annulus between the flame tube and outer casing was investigated. Tests were made to ascertain the effect of the gas nozzle position on the condition of the combustion gases.

ACKNOWLEDGEMENTS

The author wishes to express his appreciation for the assistance given him by many people in the preparation of this report. He thanks particularly Dr. J. H. T. Wade for his generous advice and guidance and Mr. G. Slinn of Orenda Ltd., Malton, Ontario for information and advice leading to the preliminary design. Thanks are also due to Mrs. A. Woodrow for her painstaking typing of the final draft.

The project was supported by Defense Research Board Grant, Number 9552-03.

CONTENTS

LIST OF ILLUSTRATIONS

NOMENCLATURE

Capitals

A	Any Area, sq. ft.
C	Heat Transferred by Convection Btu/hr,sq. ft. °R
C_d	Discharge Coefficient
D	Diameter, ft.
F	View Factor
K_c	Equilibrium Constant
M	Mass Flow Rate, lbm/sec
Nu	Nusselt Number
P	Stagnation Pressure, p.s.i.a.
ΔP	Difference in Stagnation Pressure, p.s.i.a.
Pr	Prandtl Number
Re	Reynolds Number
R	Universal Gas Constant, ft-lbf/lbm °R
R	Heat Transferred by Radiation, Btu/hr.sq. ft. $^\circ R^4$
T	Absolute Temperature, °R
ΔT	Difference in Absolute Temperature, °R
U	Velocity, ft/ sec
V	Calibrated Rotameter Reading, cu.ft/min.
Y	Penetration Distance, ft.
Z	Air Fuel Ratio

Lower Case

d	Diameter, ft
e	Emissivity
f	Fraction of Theoretical Fuel Required for Stoichiometric Combustion
g	Acceleration due to gravity, ft/sec^2
h	Heat Transfer Coefficient, Btu/hr.sq.ft. °R
k	Thermal Conductivity, Btu/hr.ft. °R

l_b	Mean Beam Path Length, ft
m	Mass Flow Rate, lbm/sec
n	Number of Dilution Air Holes Per Row
p	Static Pressure, p.s.i.a
q	Dynamic Pressure, p.s.i.
y	Excess Air

Greek Letters

β	Swirler Blade Angle
δ	Correction Factor
α	Absorbtivity
ρ	Density, lbm/cu. ft.
μ	Viscosity, lbm/ft.sec.
σ	Stefan Boltzmann Constant, Btu/hr.sq.ft.°R^4
η	Combustion Efficiency
ω	Degree of Dissociation
π	3.1416

Suffices

a	Air
an	Annulus Air
dil	Dilution Air
ft	Flame Tube Gases or Flame Tube
w	Flame Tube Wall
c	Outer Casing
ref	Outer Casing
h	Dilution Holes
sw	Swirler
st	Stoichiometric Conditions
2	Inlet Air Conditions
3	Outlet Conditions

I. INTRODUCTION

The possibility of direct power conversion using magnetohydrodynamic generation has of late been studied seriously by several American associations. Different geometric configurations of M.H.D; generators are possible, but the two which are most likely to be used are the linear channel type and the vortex flow type. The latter has certain advantages for small power outputs, and is being considered for space applications.

In order to have coupling between the fluid flow field and an applied magnetic field, it is necessary for the fluid to have a reasonably high electrical conductivity. High conductivities can be obtained if the working fluid is heated to a very high temperature, but such temperatures are destructive to the materials available at the present time. Accordingly, it has been suggested to seed combustion gases with certain additives, which by virtue of their low ionization energies, reduce the required temperature of ionization and enhance the overall conductivity of the combustion gases.

It is the purpose of this study to construct and conduct preliminary tests on a propane-air combustion system, which would provide combustion gases and be used in conjunction with a jet driven compressible vortex generator designed and tested by Trick (1).

2. LITERATURE REVIEW

Although this report is primarily concerned with the design and construction of a propane-air combustion system, it is felt some mention must be made of the ultimate object of the project, of which this report is a part.

The conversion of heat to electric power by the use of magnetohydrodynamics is an idea that has been in existence for many years. It makes use of Faraday's law of electro-magnetic induction, whereby if a conductor and a magnetic field are allowed to move relative to each other, a potential difference is induced. This conductor need not be of any special form, but the idea of using a fluid constitutes the phenomenon of magnetohydrodynamics. This phenomenon involves the use of no moving parts, but until recently, when the necessary understanding and knowledge of the performance of gases at high temperature appeared, no forms of the idea ever made much advance.

The principal problem is the coupling between the fluid flow field and the applied magnetic field, as it is necessary for the fluid to have a reasonably high electrical conductivity. The problem of gas conductivity and temperature requirements are fully considered by Rosa (2). He points out that reasonable conductivities are obtained at temperatures above 2000°R and this is borne out by the experimental data in Reference (3). The temperatures obtained in the latter, using a propane-air system are of the same order as have been obtained in this report.

Sporn and Kantrowitz (4) consider the question of magnetohydrodynamics as a future power process, and although they do not commit themselves to a definite date, they do state that power could be produced at a competitive cost, and at higher thermal efficiencies than in a steam boiler for example (in the order of 60%), but the future as a whole is largely uncertain.

Lewellen and Grabowsky (5) point out the need for a lightweight electrical power supply capable of producing power for a long time in the field of space exploration. The requirements for a long period of operation dictates a closed cycle system, and hence heat rejection by radiation, which is more effective at high temperatures. The use of an M.H.D. converter, allows the temperature of the whole system to be raised, and thus greatly improving performance. They compare vortex and linear generators, and point out that the vortex configuration allows a long interaction time, while the physical dimensions are kept small.

Although nuclear energy would probably be the power source for a practical M.H.D. converter, a study was done by Mullaney and Dibelius (6) on a linear power generator using combustion gases as the energy source. They used a flame gas temperature of 2300°K, and potassium carbonate (1 to 6% by weight of combustible mixture) as the additive. The power output was found to be 55% of the theoretical value, and the discrepancy was believed due to the velocity and temperature gradients in the power extraction channel. The results obtained, however, do point to the possibility of reasonably efficient power generation in a vortex system.

The number of papers dealing specifically with the problem of combustion chamber design are very few. Lefebvre and Herbert (7) consider the derivation of the flame tube temperature, and the effect of chamber variables on this temperature, some of which are presented later in this report. The method they follow is essentially that described in the section dealing with cooling air requirements. Clarke (8) deals with the problems associated with the aero gas turbine and first considers flame stabilization and heat release rate and the effect of air-fuel ratio, altitude and flow pattern on these parameters. He compares the tubular, tubo-annular and annular chambers in great detail, and then considers the many combustion problems associated with varying inlet conditions.

Both these preceding papers were incorporated in the unpublished material that was obtained from Orenda Limited, Malton, Ontario; Reference (9). The design of the combustion chamber was effected by reference to this material, and follows a standard procedure.

3. Design of The Combustion Chamber

3.1 Basic Considerations

A wide range of requirements, which are by no means compatible, must be satisfied in the design of a combustion chamber. The design must be effected by giving due consideration to the importance of high efficiency and stability of combustion, low losses, good outlet temperature profile, minimum initial cost, maximum endurance, and economical operation and maintenance, relative to the system of which the combustion chamber is to be a part.

In an academic fashion one may consider the conbustion as taking place in a constant area duct as shown in Figure 1A. This simple system has several disadvantages in actual practice. For example the inlet mass flow, as taken from an axial compressor provides very high gas velocities, of the order of 500 ft/sec. Flame propagation velocities are typically an order of magnitude less than this and so some form of diffuser must be added to obtain lower velocities in the combustion chamber as shown in Figure 1B. In practice it has also been found necessary to provide some type of stagnation zone in the combustion region to stabilize the combustion process and this is normally obtained by the insertion of a bluff body as shown in Figure 1C. The stagnation region behind the body provides a quiscent region wherein the flame kernel can develop and propagate into the unburnt mixture.

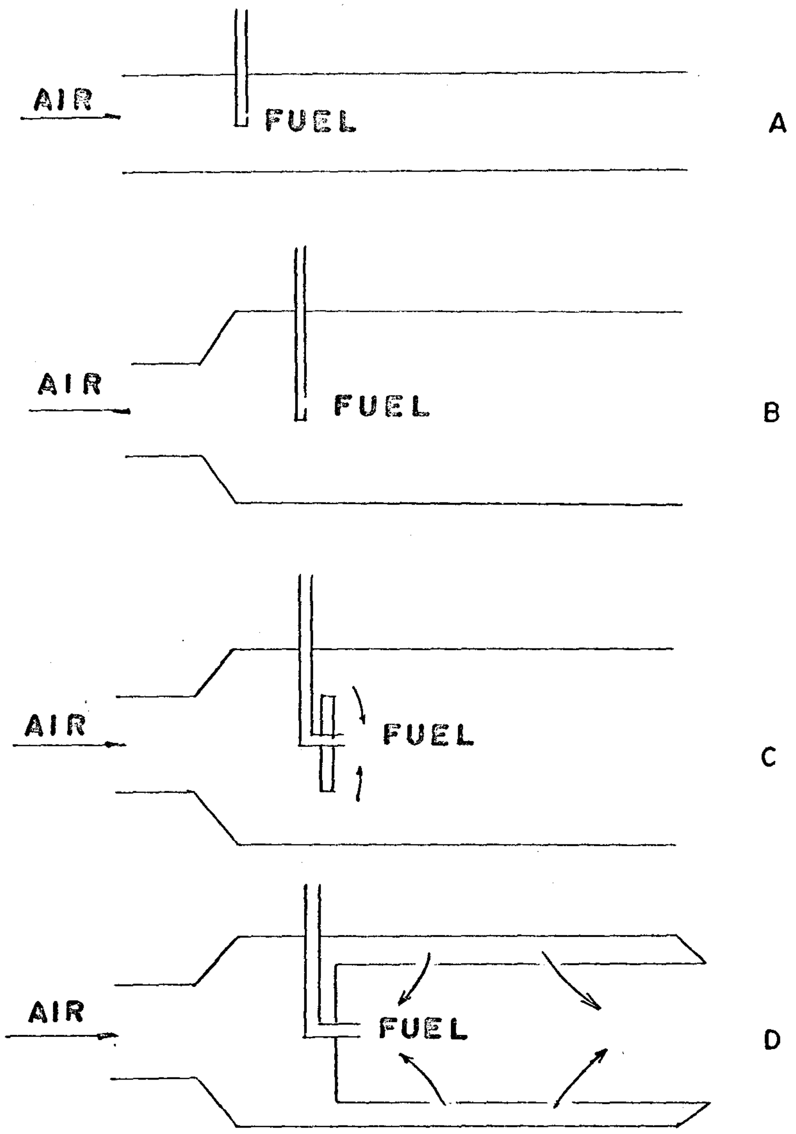

FIGURE 1

The Developement of the Conventional Combustion Chamber

A final modification must be made as a result of the limits on the air-fuel ratio which are required for a combustion process. The stoichiometric air-fuel ratios for hydrocarbon fuels are approximately 15, while the limits of flammability lie between 8 and 30. In most applications this requires that only a part of the initial mass flow be used directly in the combustion process, the remainder of the air bypassing the combustion process to provide cooling of the combustion chamber as required and more important to dilute the hot gas stream from the combustor so that the maximum temperatures entering the turbine or exhaust system are within the metallurgical limits of the system. The basic combustor system is then as shown in Figure 1D.

The flame tube is conventionally divided into three zones, as in the sketch shown here:-

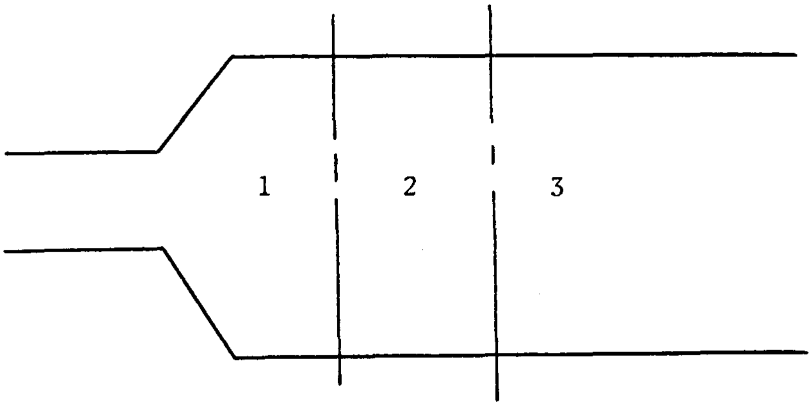

The first zone, number 1, is the primary zone, where the air and fuel are added in an approximately stoichiometric mixture, and where most of the combustion takes place. The second zone, number 2, is the intermediate zone, where a small amount of air may be added to reduce the temperature of the combustion products, and to recover some of the heat lost due to dissociation. The rest of the air is added in the dilution zone, number 3, in order to reduce the gas temperature to an acceptable level.

The distribution of air is dictated by the requirements of the combustion system, and in this design no allowance was made for air to enter the intermediate zone, and the flow was divided equally between the dilution zone, and the primary zone. The configuration of the chamber is shown in Figure 2.

In order to initiate a combustion chamber design, the requirements of the turbine, or downstream section must be known, as must the condition of the fuel and air at inlet. Attention should be paid to weight and space limitations, and the properties of the fuel should also be known. The pressure loss through the system should be kept to a minimum, while the combustion efficiency should be as high as possible.

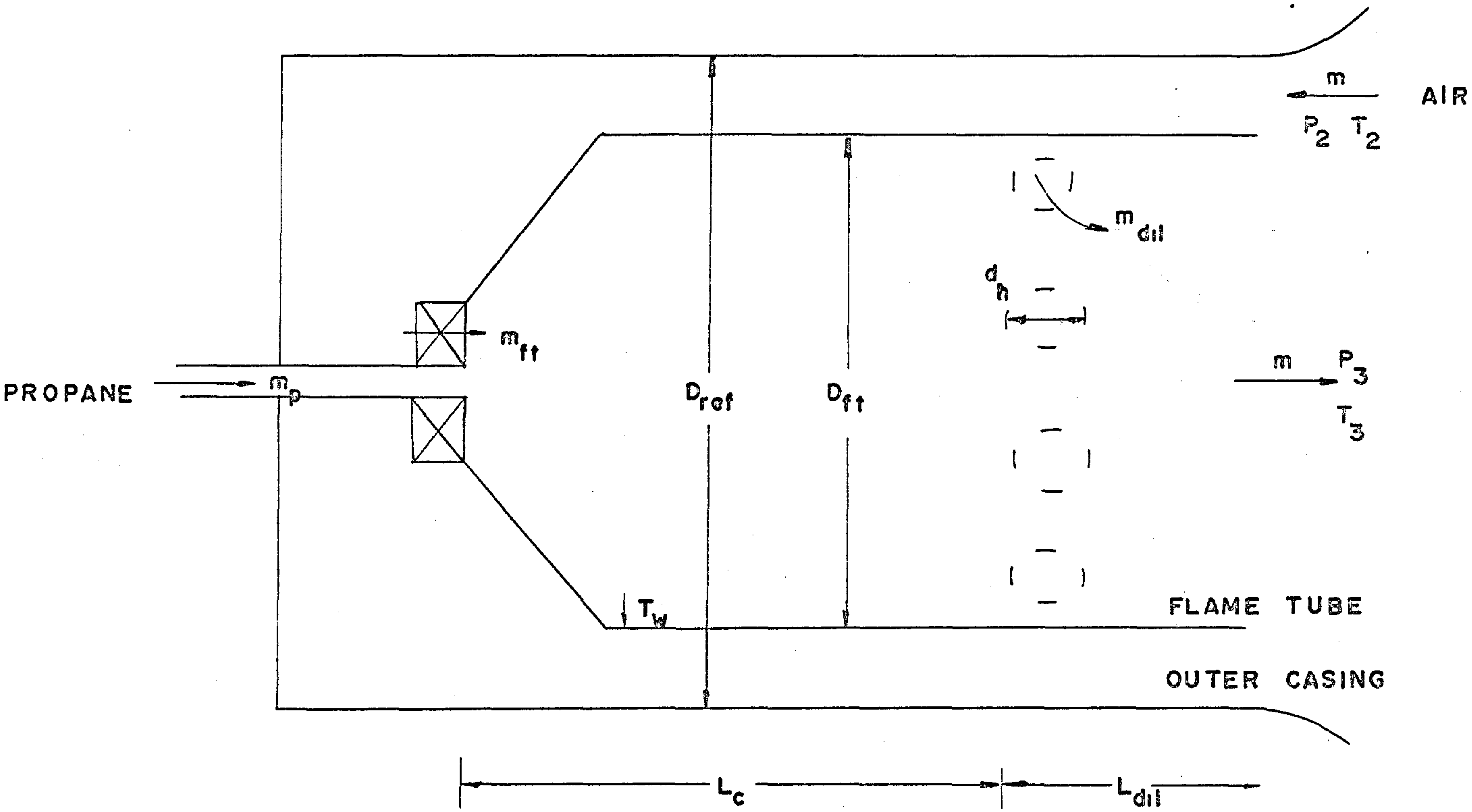

FIGURE 2

Combustion Chamber Configuration

The design variables which must be considered, and which are discussed later in Section 3.3 are:-

i) combustion chamber type

ii) dimensions of component parts

iii) primary air-fuel ratio

iv) air flow distribution and penetration

v) fuel injection

vi) ignition equipment

vii) fuel atomization, evaporation in the case of liquid fuels, carbon formation and ash deposition.

The combustion efficiency η, an important parameter, is defined, for a given geometry and air-fuel ratio, as a function of $\left(\frac{\text{residence time}}{\text{mixing time + reaction time}}\right)$ and must be considered in the calculation of the flame temperature. The residence time is taken as the time the air-fuel mixture resides in the flame tube. The mixing time is the time that it takes for the air and fuel to reach a condition conducive to ignition, while the reaction time is that time the chemical combustion reaction needs to go to completion. At low pressures the reaction time is longer than the mixing time, and combustion performance depends on chemical considerations. As the pressure is increased, the reaction time is reduced and turbulent mixing and fuel evaporation become important. Dissociation effects in the primary zone, where the temperature is high enough, lead to combustion inefficiency.

Recombination can, however, be effected at lower gas temperatures by admitting a small amount of air into the intermediate zone. If this is not done, the dissociation products become chilled on contact with the cold dilution air, which again reduces the efficiency of combustion.

3.2 Dimensional Analysis:

In the design of many systems involving fluid flow, it is often useful to perform experiments on scale models in order to predict the performance of the original. It is, however, normally impossible to scale down all the component processes in a combustion chamber, since the similarity requirements are mutually incompatible, but it can be done under the following conditions:-

i) Geometric similarity
ii) Constant Reynolds number
iii) Constant ratio of residence to combustion time

The principal restrictions are:-

i) Low Mach number
ii) Negligible heat losses
iii) Negligible effect of combustion rate on processes of fuel injection, atomization and evaporation.

The air and fuel flow patterns can be studied by use of a water analog, so as to be able to predict efficient mixing and penetration of the dilution air.

3.3 Design Method:

The design is effected by isolating the component processes, which are tabulated in Figure 3, and which are each described for the design of the combustion chamber used in this report.

A. Flame Tube Area:

If we choose an arbitrary velocity in the flame tube of 10 ft/sec., a figure recommended by past experience, and with the density of the air given by

$$\rho_2 = \frac{P_2}{RT_2}$$

$$= \frac{85 \text{ x } 144}{53.3 \text{ x } 530}$$

$$= 0.434 \text{ lbm/ cu. ft.}$$

we have, using one dimensional theory

$$A_{ft} = \frac{m_{ft}}{\rho_2 U_{ft}}$$

$$= 3.5 \text{ sq. in.}$$

As a swirler is being used at the entrance to the flame tube, a discharge coefficient, defined as the ratio of the actual velocity to the theoretical velocity, is allowed for and is given an arbitrary value of 0.75. Hence the required area for the flame tube is

$$A_{ft} = 4.67 \text{ sq. in.}$$

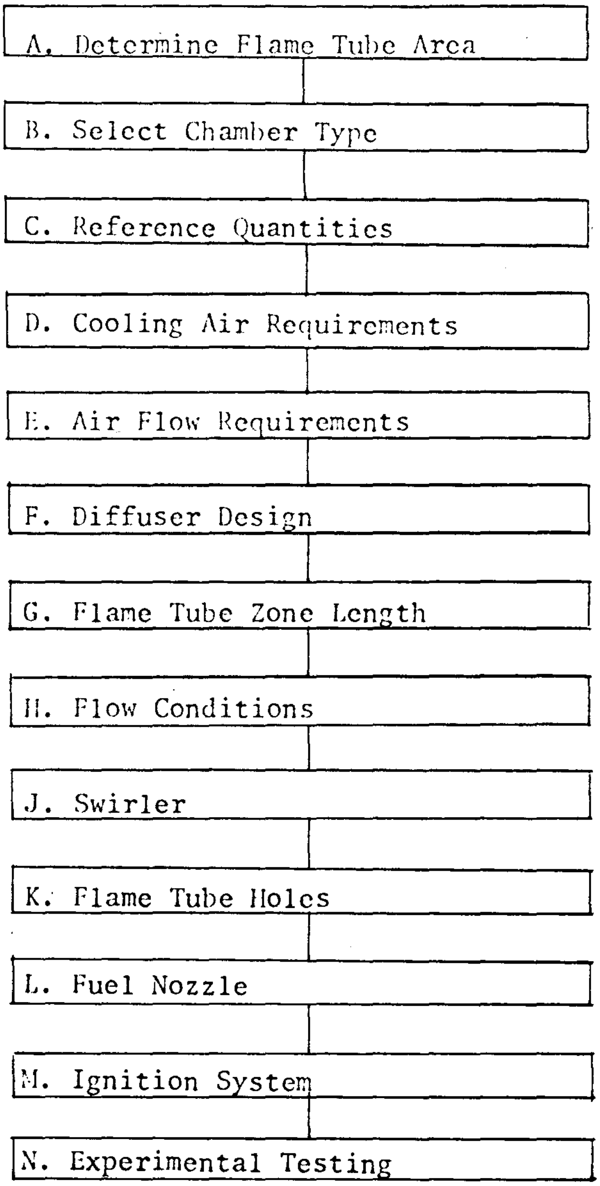

FIGURE 3

Combustion Chamber Design Steps

Hence, the flame tube diameter is 2.44 inches and as the annular duct, between the outer casing and the flame tube, carries the same mass flow, it needs the same area. To satisfy these requirements and for ease of construction, the flame tube diameter was made 3 inches and the outer casing diameter 4 inches.

B. Chamber Type:

The three normal types of single chamber, as shown in Figure 4, are

i) tubular
ii) tubo annular
iii) annular

The tubular construction was chosen as it is easy to make, has a high resistance to buckling, and the fuel and air flow patterns are easily matched, while the primary zone air flow characteristics are good. The main disadvantages are inefficient space utilization, high weight and with the reverse flow configuration, relatively high pressure losses. The layout of the reverse flow chamber used is shown in Figure 16.

C. Reference Quantities:

The reference quantities that need to be known are

i) the mean velocity

$$U_{ref} = \frac{R\, m\, T_2}{A_{ref}\, p_2}$$

$$= \frac{53.3 \times 0.3 \times 530}{12.57 \times 85}$$

$$= 7.94 \text{ ft/sec.}$$

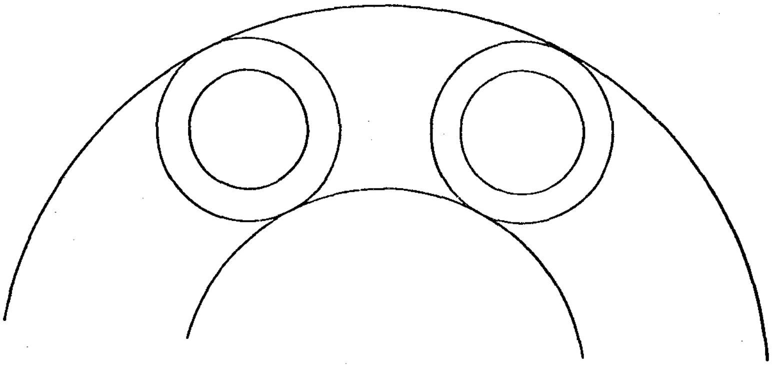

TUBULAR CHAMBER

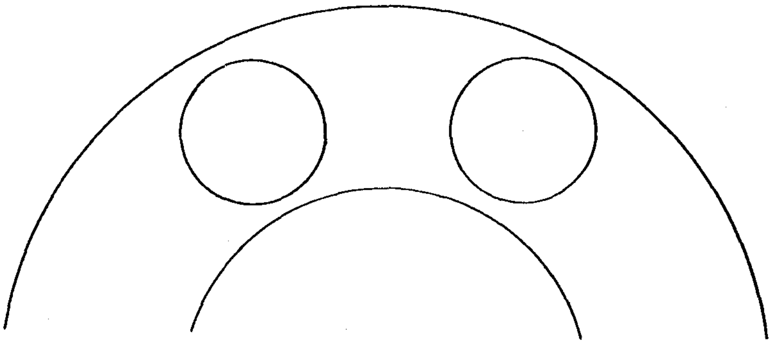

TUBO ANNULAR CHAMBER

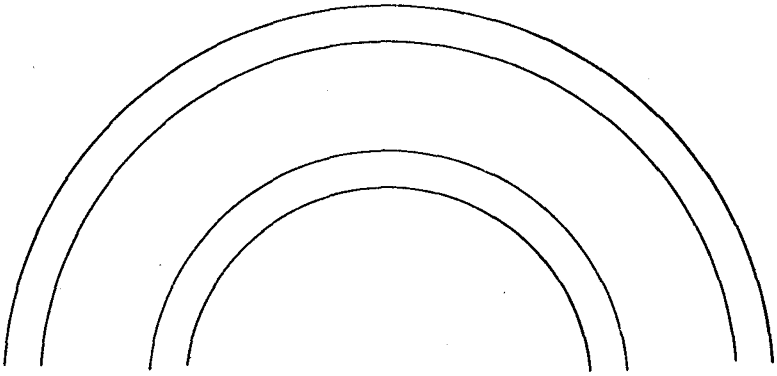

ANNULAR CHAMBER

FIGURE 4

End View of the Three Types of Combustion Chamber

ii) the dynamic pressure, referred to inlet conditions

$$q_{ref} = \frac{\rho_2 U_2^2}{2g}$$

$$= 0.425 \text{ lbf/ft}^2$$

where U_2 is calculated using the cross-sectional area of the outer casing.

iii) the pressure loss coefficient

$$\frac{\Delta P_{2-3}}{q_{ref}} = \frac{\Delta P_{2-3}}{P_2} \cdot \frac{P_2}{q_{ref}}$$

$$= 576$$

where $\frac{\Delta P_{2-3}}{P_2}$ is taken as a 2% loss, and is a representative figure based on modern practice.

D. Cooling Air Requirements

D.1 In order to determine whether any cooling is needed, an estimation must be made of the temperature of the components. The most important is the temperature of the flame tube wall, for its life, and therefore that of the system, is determined by the mechanical and thermal stresses it has to undergo. Any buckling that occurs will upset the cooling mechanism, and aggravate overheating and distortion. High temperature enhances oxidation, which reduces mechanical strength. The thermal and mechanical stresses are most serious in transition and may fluctuate between wide limits. The flame tube wall temperature under operating conditions must be calculated, and if too high, reduced to an acceptable level.

In order to calculate the wall temperature, consider the heat balance between radiation and convection to the flame tube wall from the hot gases, and from the wall to the outer casing. The following relation holds

$$R_1 + C_1 = R_2 + C_2$$

where R denotes the net rate of radiative heat transfer, and C the net rate convective heat transfer. Suffix 1 denotes from the hot gases to unit area of the flame tube wall, and suffix 2 denotes from unit area of the flame tube wall to the outer casing.

Any other components of heat transfer to and from the flame tube wall are negligibly small, and can be justifiably ignored in most practical cases.

D.2 Radiation Heat Transfer

The radiation R_t from a black body, at a temperature T, is given as

$$R_t = \sigma T^4$$

where σ is the Stefan Boltzmann constant and is equal to 1.72 x 10^{-9} Btu/hr. sq.ft°R^4.

From an actual object, the radiation at a wave length λ

$$R = e_\lambda (R_\lambda)_{\text{black body}}$$

where e_λ is the emissivity at wave length λ and the total radiation is then

$$R = \Sigma e_{\lambda}(R_{\lambda})_{\text{black body}}$$

For a grey body, e_t is defined as being equal to e_{λ}, and to be a constant. Hence if the flame is considered to be a grey body, the radiation emitted from it is then

$$R_{ft} = \sigma e_{ft} T^4_{ft}$$

and the radiation emitted from the wall, also considered to be a grey body, is

$$R_w = \sigma e_w T^4_{ft}$$

The net radiation interchange from the flame to the wall is

$$R_1 = \sigma(e_{ft} T^4_{ft} - e_w T^4_w)$$

However, a fraction α_w is absorbed and $1 - \alpha_w$ reflected, but that portion reflected passes through the flame and is again incident on the wall, so an effective absorbtivity is defined as

$$\alpha^1_w = 1/2(1 + \alpha_w)$$

giving

$$R_1 = 1/2\ \sigma(1 + \alpha_w)(e_{ft} T^4_{ft} - e_w T^4_w)$$

After considering a wide range of values Lefebvre and Herbert (7) state that to a sufficiently close approximation

$$\frac{e_w}{e_{ft}} = \left(\frac{T_{ft}}{T_w}\right)^{1.5}$$

Hence

$$R_1 = 1/2\ \sigma(1 + \alpha_w)\ e_{ft}\ T_{ft}^{1.5}\ (T_{ft}^{2.5} - T_w^{2.5})$$

Following a similar argument, where account is taken of the multiple reflections and absorbtions between the outer casing and the flame tube

$$R_2 = \sigma(1 - \alpha_{an})\left[\frac{e_w\ e_c}{e_w e_c(\frac{1}{F_{wc}} - 1) + e_c + e_w(1 - e_c)\ \frac{A_w}{A_c}}\right](T_w^4 - T_c^4)$$

It was assumed that the wall temperature is constant along the length of the flame tube and the outer casing. F_{wc} is the shape factor, and represents the fraction of the total radiant energy leaving the flame tube that is intercepted by the casing. The heat transferred by radiation is usually equal to less than one quarter of the convective heat, and the following approximations from Reference 9 can be made

i) the casing temperature T_c is equal to the inlet air temperature T_2

ii) the shape factor F_{wc} for two concentric cylinders, and neglecting end effects, is close to unity, and the term containing it can be omitted

iii) the annulus air is almost transparent to radiation, and hence $1 - \alpha_{an} = 1$

Therefore

$$R_2 = \sigma\left[\frac{e_w\ e_c}{e_c + e_w(1 - e_c)\ \frac{A_w}{A_c}}\right](T_w^4 - T_2^4)$$

D.3 Convective Heat Transfer

Convective heat transfer is defined as

$$C = h\Delta t$$

and hence

$$C = h_{ft-w} (T_{ft} - T_w)$$

The heat transfer coefficient h_{ft-w} comes from the following relationship

$$Nu = k_i Re^{k_2} Pr^{k_3}$$

where $k_i = 0.02 - 0.03$

$k_2 = 0.8$

$k_3 = 0.2 - 0.4$

Humbles (10) gives

$$Nu = 0.023 \, Re^{0.8} \, Pr^{0.4} \left(1 + \left(\frac{L}{D_{ft}}\right)^{-0.7}\right)$$

where Nu is the average Nusselt Number for the heat transfer at a tube wall, from the entrance to a position corresponding to length L, and takes account of developing boundary layer. In the intensely turbulent conditions in the flame tube, the concept of a developing boundary layer is not relevant, and it is best to use

$$Nu = 0.023 \, Re^{0.8} \, Pr^{0.4}$$

This gives

$$C_1 = 0.023 \frac{K_{ft}}{D_{ft}} Re^{0.8} \, Pr^{0.4} (T_{ft} - T_w)$$

For the convective heat transfer from the wall to the casing, the same considerations apply but none of the available data suits the problem exactly.

McAdams (11) recommends

$$Nu = 0.023\ Re^{0.8} Pr^{0.33} \left(\frac{\mu_{an}}{\mu_W}\right)^{0.14} \left(1 + 2.3\ \frac{D_{an}}{L}\right)$$

Montgomery and Weiss (12) give

$$Nu = 0.023\ Re^{0.8} Pr^{0.4} \left(\frac{D_{out}}{D_{inner}}\right)^{0.45}$$

while Judd and Wade (13) recommend

$$Nu = 0.02\ Re^{0.8} Pr^{0.33} \left(\frac{D_{out}}{D_{inner}}\right)^{0.5}$$

The Nusselt and Reynolds numbers are based on the hydraulic diameter of the annulus, and all the gas properties are evaluated at the bulk air temperature. Reference 9 recommends the last equation, and therefore

$$C_2 = 0.02\ \frac{K_{an}}{D_{an}}\ Re^{0.8} Pr^{0.33} \left(\frac{D_{ref}}{D_{ft}}\right)^{0.5} (T_W - T_2)$$

D.4 Flame Emissivity

In order to calculate the radiation leaving an object it is necessary to know the emissivity of that object. In the case of a flame, an~~d~~ accurate determination is impossible, and the concept of a mean beam path length has been introduced. This is defined as the radius of an equivalent gas hemisphere, radiating to a small surface of unit area at the centre of its base. For a cylindrical enclosure of diameter equal to its base, Kreith (14) gives

$$l_b = 0.6 \times \text{diameter}$$

and for an infinitely long cylinder

$$l_b = \text{diameter}$$

In this case, l_b lies between the two, and Hottel (15) gives

$$l_b = 3.6 \left(\frac{\text{volume}}{\text{surface area}}\right)$$

The emissivity of the flame is quoted, in Reference 9 as

$$e_{ft} = 1 - \exp(-3.9 \times 10^4 L p_2 \left(\frac{\ell_b}{Z_{st}}\right)^{0.5} T_{ft}^{-1.5})$$

where L is the luminosity correction and

$$L = \exp\left(\frac{C/H - 4.4}{2.3}\right)$$

where C/H is the ratio of the weight of carbon to hydrogen in the fuel, and for propane is equal to 4.5.

D.5 Calculation

We have

$$R_1 + C_1 = R_2 + C_2$$

$$1/2\ \sigma(1+\alpha_w) e_{ft} T_{fc}^{1.5} (T_{ft}^{2.5} - T_w^{2.5}) + 0.023 \frac{K_{ft}}{D_{ft}} Re^{0.8} Pr^{0.4} (T_{ft} - T_w)$$

is equal to

$$\sigma\left(\frac{e_w e_c}{e_c + e_w(1-e_c)\frac{D_{ft}}{D_{ref}}}\right)(T_w^4 - T_2^4) + .02 \frac{K_{an}}{D_{an}} Re^{0.8} Pr^{0.33} \left(\frac{D_{ref}}{D_{ft}}\right)^{0.5} (T_w - T_2)$$

which can be written as

$$AT_w^4 + BT_w^{2.5} + (C_{an} + C_{ft})T_w = AT_2^4 + BT_{ft}^{2.5} + C_{ft}T_{ft} + C_{an}T_2$$

The properties of the gas for the convective heat transfer are evaluated at the flame temperature for the internal convection, and at the air inlet temperature for the internal convection.

The flame temperature is obtained by considering data from Figures 5, 6, 7. Figure 5 shows the adiabatic temperature rise due to combustion for a fuel type JP4, with a lower calorific value of 18,540 BTU/lbm, against the fuel air ratio in the combustion zone. These results are valid for one atmosphere pressure, and as the intended air inlet pressure is five atmospheres, a correction must be made. Figure 6 gives a co-rection factor to be applied to the data on Figure 5, to give the temperature rise at ten atmospheres. The algebraic mean of the two values is used for a pressure of 5 atmospheres. Consider a stoichiometric mixture

$$\frac{1}{Z_{st}} = \frac{1}{15.72} = 0.067$$

where Z_{st} is the stoichiometric fuel air ratio. Now

$$\begin{aligned} \Delta T &= 3240°R \text{ at 1 atm} \\ &= 3300 \times 1.02 \\ &= 3300°R \text{ at 10 atm} \end{aligned}$$

Therefore at 5 atm

$$\Delta T = 3270°R$$

Assuming a combustion efficiency η of 0.8, a figure which is given in Lefebvre and Herbert (7) for conventional combustion chambers, and applying the correction factor δ, for a fuel of different lower calorific value, which for propane is 1.05, the flame temperature is

$$\begin{aligned} T_{ft} &= T_2 + \eta\delta\Delta T°R \\ &= 530 + 1.05 \times 0.8 \times 3270°R \\ &= 3280°R \end{aligned}$$

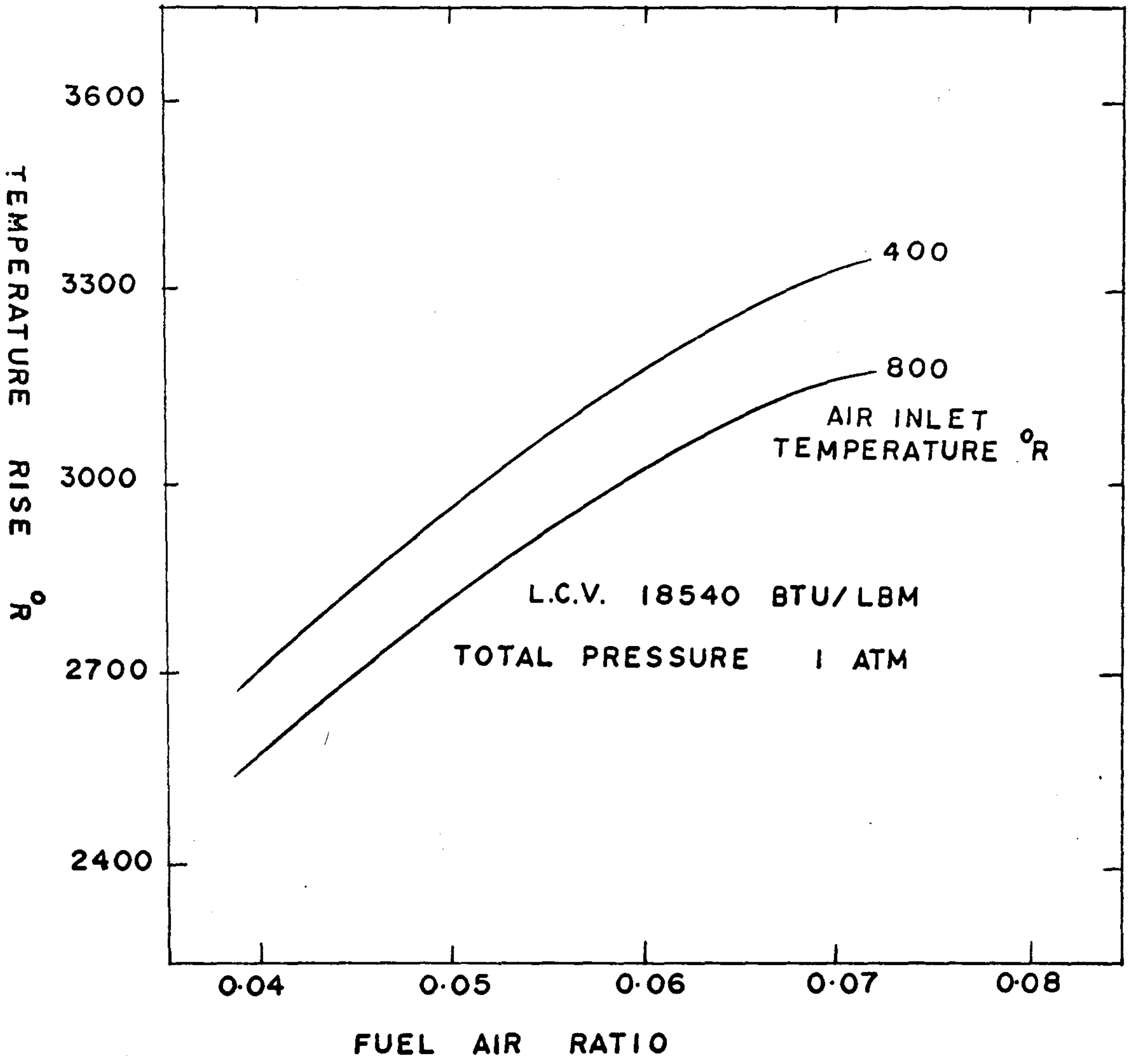

FIGURE 5

Adiabatic Temperature Rise for JP4 Type Fuel

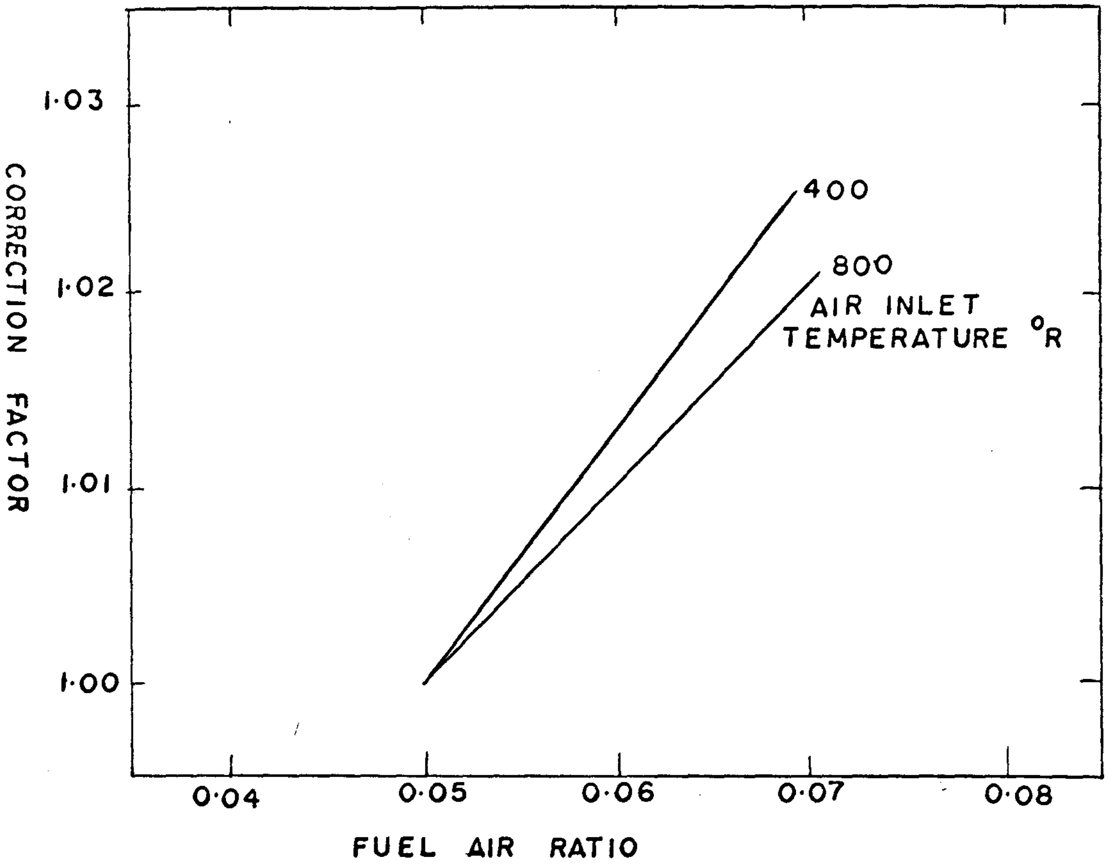

FIGURE 6

Correction Factor for JP4 Type Fuel

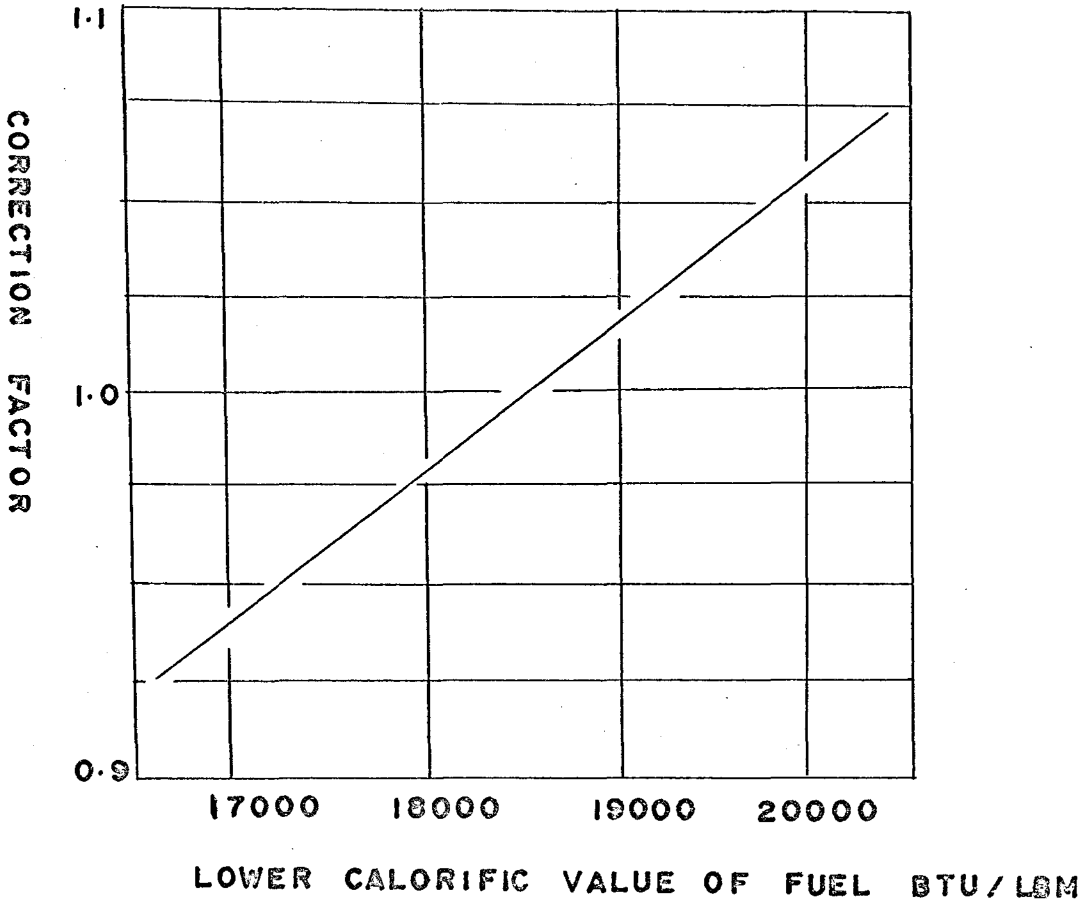

FIGURE 7

Correction Factor for Adiabatic Combustion Temperature Rise
vs Lower Calorific Value of Fuel

To evaluate the constants A and B, we need to know the emissivities involved. From Reference 9, e_w is given as 0.7 for a nimonic, and Kreith (14) gives e_c as 0.8 for a stainless steel. Now

$$e_{ft} = 1 - \exp\left(-3.9 \times 10^4 L p_2 \left(\frac{\ell_b}{Z_{st}}\right)^{0.5} T_{ft}^{-1.5}\right)$$

$$L = \exp\left(\frac{C/H-4.4}{2.3}\right)$$

$$= 1.0445$$

$$p_2 = 5 \text{ atm}$$

$$l_b = 3.6\left(\frac{\pi \times 3 \times 3 \times 9}{4\pi \times 3 \times 9 \times 12}\right)$$

$$= 0.225 \text{ ft.}$$

$$Z_{st} = 15.72$$

$$\left(\frac{l_b}{Z_{st}}\right)^{0.5} = 0.196$$

$$T_{ft}^{-1.5} = 0.538 \times 10^{-5}$$

Therefore

$$e_{ft} = 0.212$$

The emissivity can also be calculated by considering the emissivity of the main components of combustion which radiate energy, i.e. carbon dioxide and water vapour. The value obtained by using tables available in Kreith (14) and following his procedure, is

$$e_{ft} = 0.195$$

This value agrees reasonably well, and the first value which is based on experimental evidence will be used.

Therefore,

$$A = 1.72 \times 10^{-9} \left(\frac{e_w \, e_c}{e_c + e_w \, (1-e_c) \frac{D_{ft}}{D_{ref}}} \right)$$

$$= 1.06 \times 10^{-9} \text{ Btu/hr. sq. ft.}^\circ R^4$$

$$B = 1.72 \times 10^{-9} \left(\frac{1 + \alpha_w}{2} \right) e_{ft} \, T_{ft}^{1.5}$$

$$= 5.75 \times 10^{-5} \text{ Btu/hr. sq.ft.}^\circ R^{2.5}$$

Now

$$C_{ft} = 0.023 \, \frac{k_{ft}}{D_{ft}} \, Re^{0.8} Pr^{0.4} \text{ Btu/hr sq. ft.}^\circ R$$

The gas properties are evaluated at the flame temperature from data obtained from Kreith (14) and Hilsenrath and Toulovkian (16). An average value was found in each case by taking the constituent values in their proportion. The validity of this method is shown in Appendix 3. The values for the viscosity of the constituent gases are

$$\mu_{CO_2} = 4.00 \times 10^{-5} \text{ lbm/ft.sec.}$$

$$\mu_{N_2} = 4.35 \times 10^{-5} \text{ lbm/ft. sec.}$$

$$\mu_{H_2O} = 3.82 \times 10^{-5} \text{ lbm/ft. sec.}$$

These values are then taken in the ratio of the amounts of each gas in the combustion products. Hence

$$\mu_{ft} = \frac{19 \times 4.35 + 4 \times 4.00 + 3 \times 3.82}{26} \times 10^{-5}$$

$$= 4.2 \times 10^{-5} \text{ lbm/ft. sec.}$$

Following a similar argument

$$k_{ft} = 0.068 \text{ Btu/hr.ft.°R}$$

Now

$$D_{ft} = 0.25 \text{ ft}$$

and

$$Re_{ft} = \frac{D_{ft} \times m_{ft}}{\mu_{ft} \times 0.6 \, A_{ft}}$$

$$= 3.03 \times 10^{4}$$

The factor 0.6 is included to allow for recirculation and is an arbitrary value based on experimental combustion chamber performance. Reference (9) recommends that Pr = 0.7 be used for both the flame tube and the annulus. Hence

$$C_{ft} = 0.023 \times \frac{0.068}{0.25} \times 3.85 \times 10^{3} \times 0.87$$

$$= 20.9 \text{ Btu/hr. sq. ft.°R}$$

Now

$$C_{an} = 0.02 \, \frac{k_{an}}{D_{an}} \, Re^{0.8} \, Pr^{0.33} \, \left(\frac{D_{ref}}{D_{ft}}\right)^{0.5}$$

From the same considerations as above

0.0151

$$k_{an} = 0.151 \text{ Btu/hr. ft.°R}$$

$$\mu_{an} = 1.22 \times 10^{-5} \text{ lbm/ft. sec.}$$

$$D_{an} = \frac{4 \times A_{an}}{\text{Wetted Perimeter}}$$

$$= \frac{4 \times \pi(16-9)}{4\pi \times (4 + 3)}$$

$$= 1.0 \text{ in.}$$

$$= 0.0834 \text{ ft.}$$

$$Re_{an} = 2.68 \times 10^4$$

$$\frac{D_{ref}}{D_{ft}} = 1.33$$

Then

$$C_{an} = 0.02 \times \frac{0.0151}{0.0834} \times 3.47 \times 10^3 \times 0.889 \times (1.33)^{0.5}$$

$$= 13.1 \text{ Btu/hr. sq. ft.}^\circ\text{R}$$

Therefore

$$AT_2^4 = 1.06 \times 10^{-9} \times (530)^4$$

$$= 84 \text{ Btu/hr. sq. ft.}$$

$$BT_{ft}^{2.5} = 5.75 \times 10^{-5} \times (3280)^{2.5}$$

$$= 35000 \text{ Btu/hr. sq. ft.}$$

$$C_{ft}T_{ft} = 20.9 \times 3280$$

$$= 68900 \text{ Btu/hr. sq. ft.}$$

$$C_{an}T_{an} = 13.1 \times 530$$

$$= 6930 \text{ Btu/hr. sq. ft.}$$

We now require to find T_w, such that

$$AT_w^4 + BT_w^{2.5} + (C_{ft} + C_{an})\ T_w = 110914 \text{ Btu/hr.sq. ft.}$$

The value that satisfies this equation is

$$T_w = 2625°R$$
$$= 2165°F$$

The primary zone flame tube wall temperature is acceptable and within the limits of the properties of Hastelloy X*, the flame tube material. As this is so, it is not necessary to change the air flow configuration.

D.6 Effect of Chamber Variables on Wall Temperature

D.6.1 Pressure

If there is an increase in inlet pressure, at constant inlet temperature and mass flow rate, the emissivity of the flame is increased, and hence the radiation from the flame to the wall increases. There is also a slight rise in flame temperature due to the suppression of dissociation.

D.6.2 Inlet Temperature

An increase in inlet air temperature, at constant pressure and mass flow rate, causes the flame temperature to rise, and hence the radiation and the convective heat transfer from the flame to the wall also increases. At the same time the temperature difference between the wall and the cooling air is reduced, lessening the cooling effect. The flame tube temperature increases approximately the same amount as the inlet temperature.

* See Appendix 1 for the physical properties of Hastelloy X.

D.6.3 Mass Flow Rate

The convective heat transfer is proportional to the mass flow rate raised to the four-fifth power, and as the heat transferred from the flame tube to the casing is greater than that from the flame to the flame tube, there is a decrease in the flame tube temperature, with an increase in mass flow rate. The emissivity of the flame is also increased, but the overall effect is small. Figures 8,9,10, taken from Lefebvre and Herbert (7) show the effect of these parameters on flame tube wall temperature, both for the experimental and theoretical case.

D.6.4 Flame Tube Size

An increase in flame tube diameter means that the mean beam length increases, thereby raising the emissivity of the flame. This will cause an increase in the flame tube wall temperature.

D.6.5 Air Fuel Ratio

Luminous flames, caused by rich mixtures, mean an increase in the wall temperature, due to the increase in flame emissivity.

It should be noted here that the tubular configuration has the lowest flame tube wall temperature.

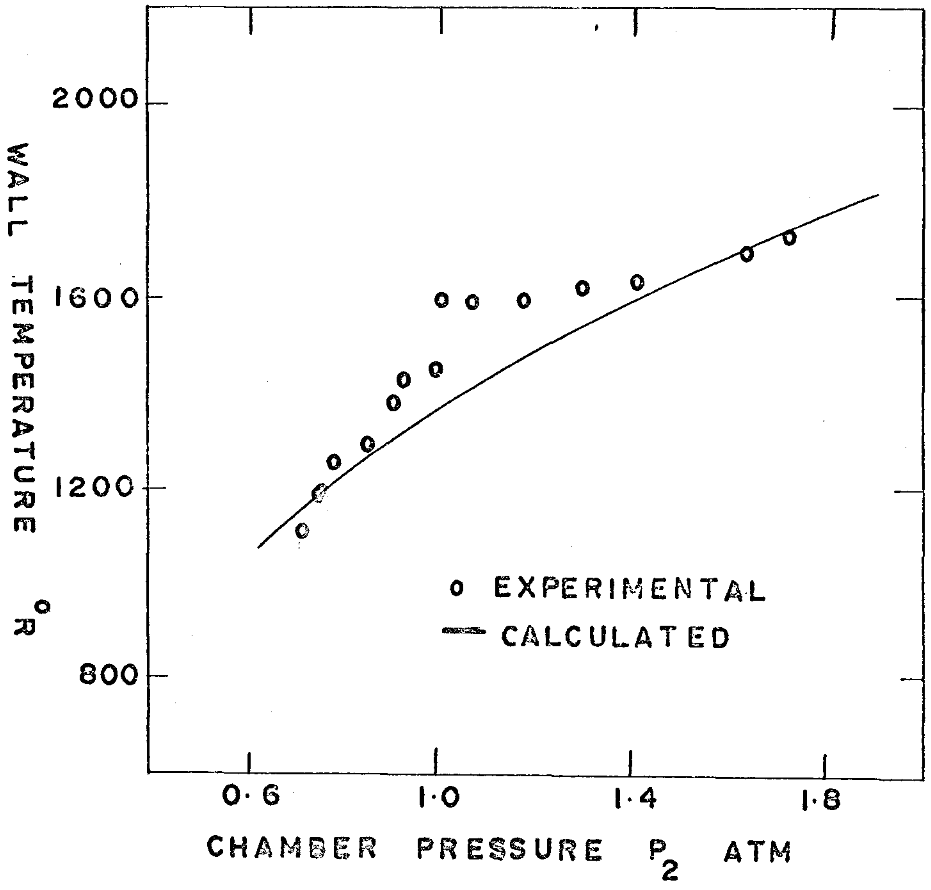

FLAME TUBE DIA 0·75 FT
D_{ref} 0·893 FT
AIR MASS FLOW RATE 2·2 LBM/SEC
T_2 = 897 °R
Z = 72

FIGURE 8

Flame Tube Wall Temperature vs Chamber Pressure

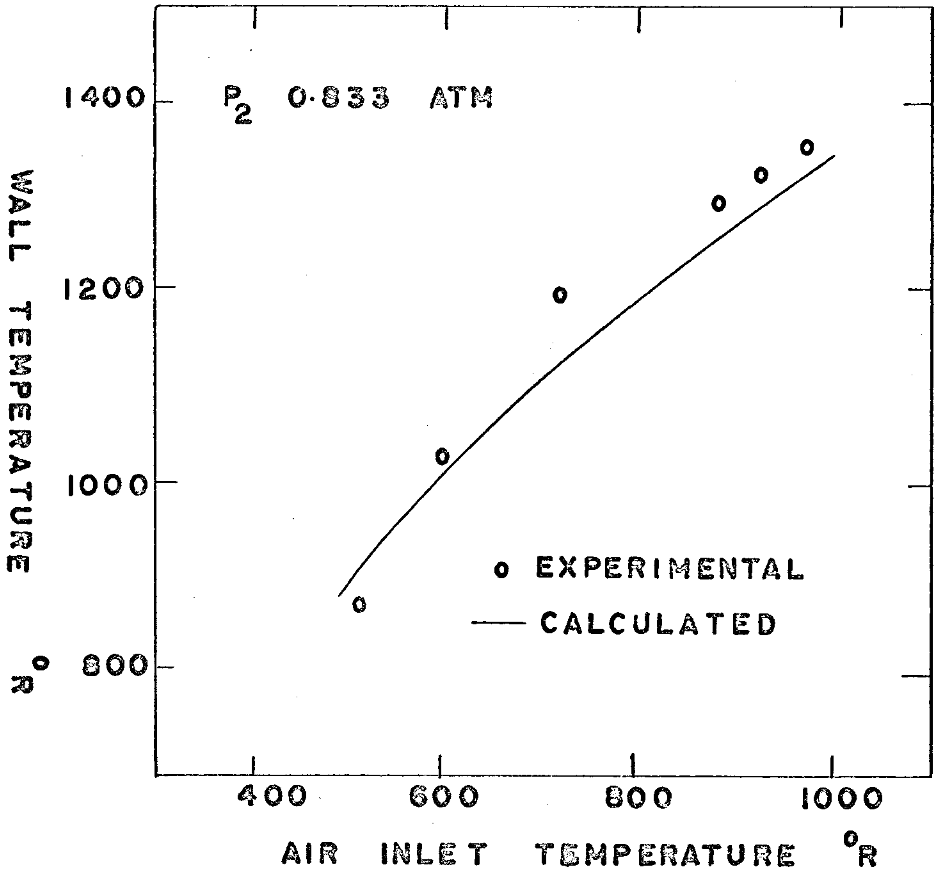

Other Data as for Figure 8

FIGURE 9

Flame Tube Wall Temperature vs
Air Inlet Temperature

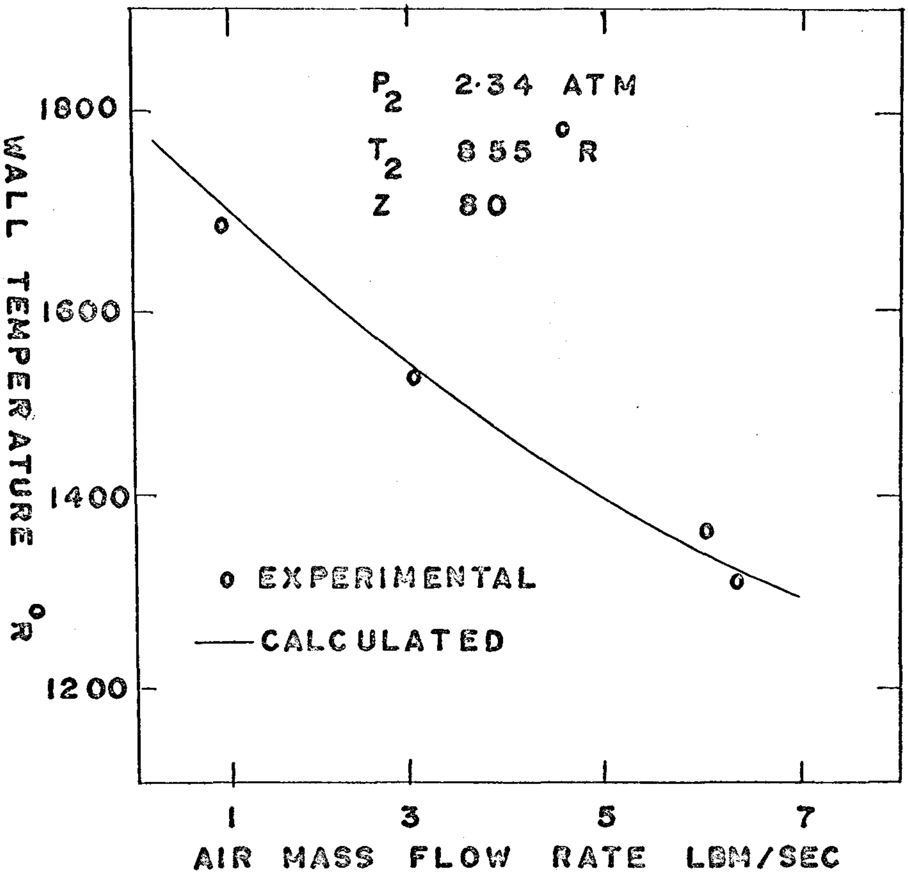

Other Data as per Figure 8

FIGURE 10

Flame Tube Wall Temperature vs
Air Mass Flow Rate

E. Air Flow Requirements

The air flow through the combustion chamber should be such that

- i) a suitable flow pattern is established for flame stability
- ii) air and fuel flow patterns are matched
- iii) the combustion products are effectively diluted
- iv) the cooling of the flame tube is effective

Furthermore, the requirements for good aerodynamic performance are a high pressure loss for adequate mixing and a low overall pressure loss for low fuel consumption. These two are incompatible and any design is therefore a compromise. In this design, it was decided to have only dilution air, with the air mass flow divided equally between it and the combustion air, and as the flame tube temperature is satisfactory, there was no need to alter this air flow pattern. The omission of secondary holes in the intermediate zone, means that the recirculation in the primary zone is not reinforced, but it was felt that the swirler would be effective enough in this respect.

In order to simplify the design a diffuser was not used and the pressure losses incurred in the chamber will come from the plenum chamber, where the flow turns through a right angle, and from the primary zone end of the annulus where the air enters the swirler. The configuration of this design makes it relatively impossible to calculate figures for the losses involved, but the skin friction losses in the annulus will be negligible compared with the loss due to the bends and the swirler. The losses due to the swirler are discussed in Section J.

F. Diffuser Design

Since no diffuser was incorporated in the design, this section is invalid.

G. Combustion and Dilution Lengths

For chambers with a single atomizer and swirler, experience shows that

$$\frac{L_c}{D_{ft}} = 1.5$$

and L_c was chosen as 4.25 inches so as to lie between the theoretical value based on the flame tube diameter calculated in Section A, and that required by the actual size of the flame tube.

The dilution length is determined by the degree of temperature uniformity required at the combustion chamber exit, and is normally chosen such that the pressure loss, which would come from good mixing is not too large. It was decided to make the dilution length about equal to the combustion length, and 5.25 inches was decided upon to allow sufficient room for the dilution air holes.

J. Swirler Design

As the flow conditions are known the swirler can be designed. Reference 9 gives the following formula for the area of the swirler.

$$\frac{m_{sw}}{m} = C_d \left(\frac{A_{sw}}{A_{ref}}\right)\left(\frac{P_{sw} - P_{ft}}{q_{ref}}\right)^{0.5} \cos \beta_{sw}$$

The turning angle β_w is equal to the blade stagger angle, which is normally between 45° and 60°, and is taken as 60°. C_d is quoted 0.85 for flat blade swirlers. The pressure drop through the swirler $P_{sw} - P_{ft}$ is assumed, for simplicity, to be one half the total pressure drop through the system

i.e. $$\frac{P_{sw} - P_{ft}}{q_{ref}} = 288$$

this gives

$$0.5 = 0.85 \times \left(\frac{A_{sw}}{A_{ref}}\right) \times (288)^{0.5} \times 0.5$$

$$\frac{A_{sw}}{A_{ref}} = 0.0405$$

$$A_{sw} = 0.509 \text{ sq. in.}$$

The nozzle was made from 5/16 inch tubing, with an area of 0.0767 sq. inches. Thus the outside diameter of the swirler is given by

$$d_{sw} = \sqrt{\frac{4}{\pi}\,(0.509 + 0.0767)}$$

$$= 7/8 \text{ inches}$$

The outer diameter is quoted as being about equal to one quarter of the flame tube diameter, that is 0.75 inches, and the value used agrees fairly well with this.

As a check on the pressure loss through the swirler, Knight and Walker (17) give

$$\frac{\Delta P_{sw}}{q_{ref}} = 1.3\ \left[\left(\frac{A_{ft}}{A_{sw}}\right)^2 \sec^2\beta_{sw} - 1\right]\ \left(\frac{m_{sw}}{m}\right)^2$$

$$= 252$$

This result would indicate that the assumption that half the pressure loss occured in the swirler is substantially correct. The swirler and the nozzle are shown in Figures 18 and 32.

K. Dilution Air

It was decided to use flush round holes for the dilution air, and a discharge coefficient is needed in order to determine the size of these holes. For the tubular configuration, C_d is defined by Dittrich and Graves (18) as

$$\frac{m_{dil}}{m}\,\frac{A_{an}}{A_{ht}} = C_d\ \left(\frac{P_{an} - P_{ft}}{q_{an}}\right)^{0.5}$$

and a value of 0.58 was obtained from Figure 11, which shows discharge coefficient as a function of pressure drop coefficient

$$\frac{P_{an} - P_{ft}}{q_{an}}$$

The next most important factor to be considered is the penetration distance of the air jet, and Hawthorne, Rogers and Zaczek (19) give

$$\frac{d_h}{D_{ft}} = \frac{0.89\ \left(\frac{Y_{max}}{D_{ft}}\right)\ \frac{U_{ft}}{U_{an}}}{\left(\frac{T_{ft}}{T_2}\right)^{0.5}\ Cd^{0.5}\ \left(\frac{P_{an} - P_{ft}}{q_{an}}\right)^{0.5}}$$

Now

$$\frac{U_{ft}}{U_{an}} = \frac{m_{ft}}{m_{an}} \cdot \frac{A_{an}}{A_{ft}} \cdot \frac{T_{ft}}{T_{an}}$$

$$= 4.79$$

We desire penetration to the centre line of the flame tube, so

$$\frac{Y_{max}}{D_{ft}} = 0.5$$

Hence

$$\frac{d_h}{D_{ft}} = \frac{0.89 \times 0.5 \times 4.79}{\left(\frac{3280}{530}\right)^{0.5} (0.58)^{0.5}\ (288)^{0.5}}$$

$$= 0.0645$$

$$d_h = 0.1935 \text{ inches}$$

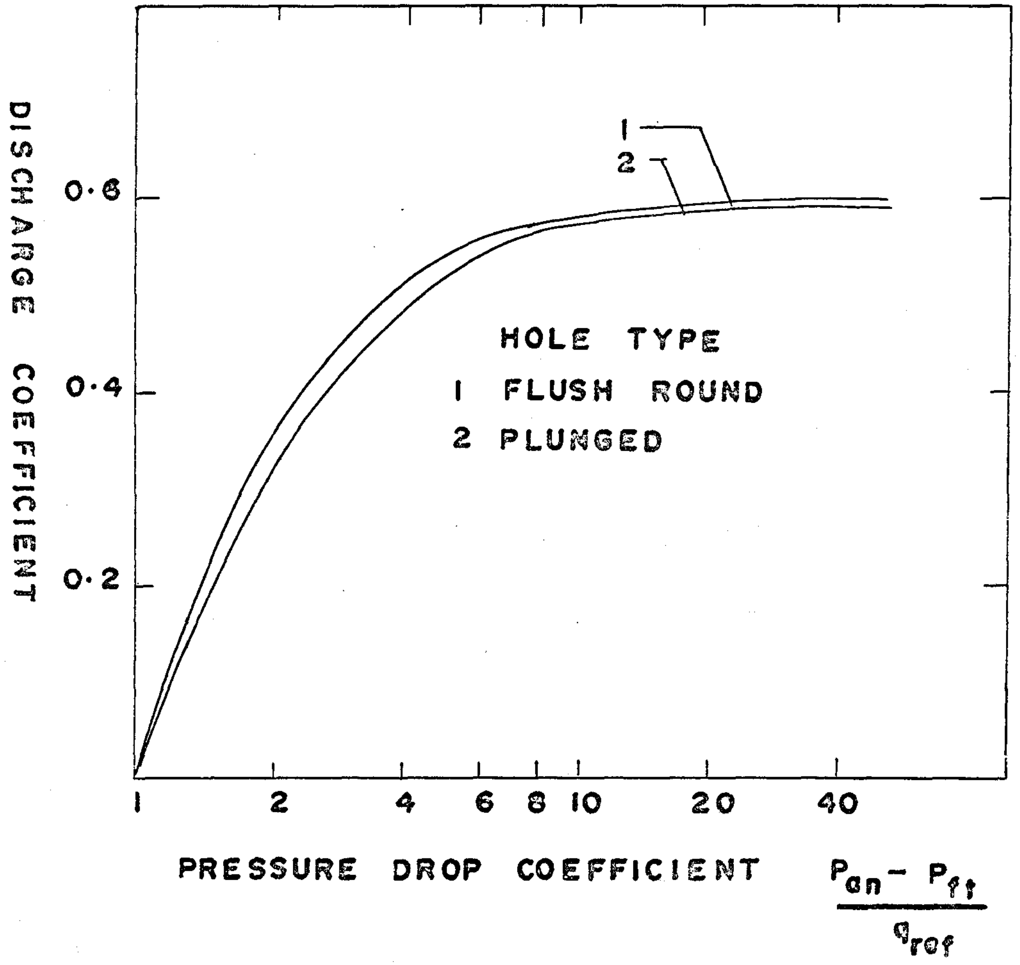

FIGURE 11

Discharge Coefficient vs Pressure Drop Coefficient for Two Hole Types

The area of one hole is therefore 0.03142 sq. inches. To get the number of holes, we have

$$\frac{n_h d_h}{\pi D_{ft}} = 0.2$$

$$n_h = 9 \text{ holes/row}$$

The mass flow is 0.15 lbm/sec and the velocity of the jet

$$u_h = \frac{2g\ P_{an} - P_{ft}}{\rho_2}$$

$$= 135 \text{ ft./sec.}$$

The required hole area is

$$A_h = \frac{m}{u_h C_d \rho_2}$$

$$= 0.635 \text{ sq. in.}$$

The number of holes required is then

$$\frac{0.635}{0.314} = 20 \text{ holes}$$

For the sake of symmetry three rows of eight holes each were used, with a hole diameter of 7/32 in.

L. Gas Nozzle Design

The main problem in injecting the gas is to obtain good mixing of the air and gas for combustion. No quantative data as to the size of the nozzle was available, and the size was arbitarily chosen giving heed to past design experience. The axial tube, with the radial holes was chosen, as it is easy to construct, and as there appears to be no particular advantage in any of the other possible types.

M. Ignition

The ignition method chosen was a high tension air-gap spark plug, which has the advantage of cheapness and long life, but needs a heavy power supply, and has poor performance at low pressures. Ignition by this method is improved with an increase in temperature, pressure, and spark energy, but any increase in gas velocity will impair the performance. In order to ignite a flammable mixture enough energy to propagate a steady combustion wave must be supplied, and during the ignition process two separate phases are gone through.

The first phase is the formation of a flame around the spark plug, of sufficient intensity so as not to be extinguished. The energy and duration of the spark, and the air-fuel ratio in the vicinity of the spark-plug determine the success of this initial phase.

The flame then travels to all parts of the primary zone, provided the air velocity, location of the spark plug, and fuel distribution are favourable.

The spark energy required for ignition depends on the strength of the mixture, and is at a minimum when stoichiometric conditions exist around the spark plug. If the temperature of the fuel is high, then less spark energy is needed, as less of that energy is absorbed by the fuel. If the air velocity in the flame tube is high then the flame cannot be sustained, and the flame is carried downstream, and extinction takes place. The recirculation zone, giving a low velocity region, provides an area where the flame can be stabilized.

Flame stability is also affected by the rate of heat release. If the heat release rate curve and the load line are plotted against the mean exit temperature, as in Figure 12, then it can be seen that as the mass flow rate is increased, the intersection of the load line, and the heat release curve moves towards higher values, until the load line becomes tangential. Any further increase in mass flow rate will extinguish the flame. For a comprehensive review of flame stabilization see Childs (20).

For any given approach condition, there exists a definite velocity, known as the blow off velocity, Haddock (21), above which the flame cannot be stabilized. The blow off velocity

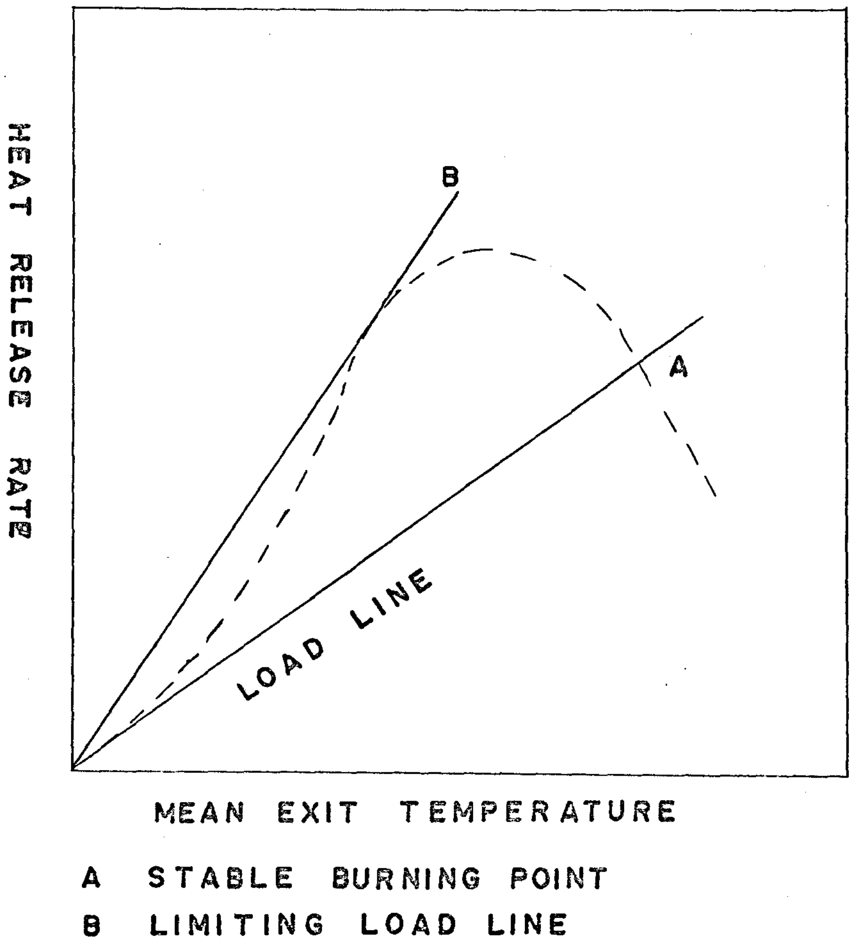

FIGURE 12

Heat Release Rate and Turbine Load Line vs Mean Exit Temperature is a function of

i) the air-fuel ratio

ii) the flame holder size and shape

iii) the temperature and pressure

iv) the nature of the fuel

The maximum blow off velocity occurs near the stoichiometric condition, and hence this is the most desirable as it is the most stable condition.

The design of the combustion chamber is now complete and it is now necessary to initiate experimental testing.

4. THEORETICAL CONSIDERATIONS

The stoichiometric combustion of a hydrocarbon fuel is defined as having all the hydrogen atoms converted to water, and all the carbon atoms to carbon dioxide, by combining with the oxygen in the air, while the nitrogen does not enter into the reaction at all. Air contains approximately 79% by volume of nitrogen and 21% by volume of oxygen, while the average ratio of the number of moles of nitrogen and oxygen in air is 3.76:1. Hence we can write the stoichiometric reaction for propane as:-

$$C_3H_8 + 5O_2 + 18.8N_2 = 3CO_2 + 4H_2O + 18.8N_2$$

This gives a stoichiometric air-fuel ratio

$$Z_{st} = \frac{5 \times 4.76 \times 28.97}{44}$$

$$= 15.72$$

The left hand side of the equation represents the theoretical mixture of reactants and the right hand side represents the theoretical composition of combustion products. In many reactions, however, excess air is present, and denoting y as the fraction of excess air, the combustion equation becomes

$$C_3H_8 + 5(1+y)O_2 + 18.8(1+y)N_2 = 3CO_2 + 4H_2O$$

$$+ 5yO_2 + 18.8\ (I+y)N_2$$

giving a theoretical air-fuel ratio of

$$Z = 15.72(1+y)$$

This analysis gives a reasonable approximation for lean combustible mixtures (excess air) at moderate temperatures and pressures with a low heat release rate. As the proportion of air in the reactant mixture is decreased to a nearly theoretical value, and in many cases to the range of rich mixtures, and/or at high temperatures, and very low pressures, the analysis becomes inadequate if reasonable accuracy is to be maintained.

The reason is that the effect of dissociation of the gases becomes more significant under these conditions. For example, at 3600°R and atmospheric pressure, 1.5% by weight of carbon dioxide is split into carbon monoxide and oxygen, while at 5400°R, 42.5% is dissociated; this information is provided by Schmidt (22). The dissociation can be explained as due to the increase in the amplitude of oscillation of the atoms in the molecule, and as the translation speed of the molecules is increased at high temperature, atoms are more easily removed when in collision.

In order to calculate the percentage of dissociation, we must consider the chemical equilibrium of the dissociation reaction, which can be understood as the state from which the reaction may proceed with the same speed in either direction.

Consider the reaction

$$\zeta_i A + \zeta_2 B \rightleftarrows \zeta_3 C + \zeta_4 D$$

At equilibrium, the following relation holds

$$K_c = \frac{[C]^{\zeta_3}[D]^{\zeta_4}}{[A]^{\zeta_1}[B]^{\zeta_2}}$$

where K_c is the equilibrium constant, and where [ ] denotes the concentration of the component.

Hence at a given temperature, the equilibrium is dependent on the proportion of the components of the gas mixture. Since in most cases, the total pressure is given, K_c can be expressed as a ratio of the partial pressures. Putting the relation $[W] = \frac{P_w}{RT}$ where W is any component and P_w its partial pressure

$$K_c = \frac{P_C^{\zeta_3} P_D^{\zeta_4}}{P_A^{\zeta_1} P_B^{\zeta_2}} \left(\frac{1}{RT}\right)^{\zeta_3 + \zeta_4 - \zeta_1 - \zeta_2}$$

$$= K_p\left(\frac{1}{RT}\right)^{\zeta_3 + \zeta_4 - \zeta_1 - \zeta_2}$$

In this study, only the dissociation of carbon dioxide, will be considered as Schmidt (22) points out that any other dissociation reaction is negligible in comparison at the temperatures we are considering.

Now $2CO_2 = 2CO + O_2$

$$K_c = \frac{P^2_{CO}\, P_{O_2}}{P^2_{CO_2}} \cdot \left(\frac{1}{RT}\right)$$

$$= \frac{r_{CO}^{2}\ r_{O_2}}{r_{CO_2}^{2}} \cdot \left(\frac{P}{RT}\right)$$

where P is the total pressure, in this case assumed to be atmospheric, and r is the proportion of the gas as a fraction of the total. If the degree of dissociation is denoted as ω, then

$$CO_2 = CO_2(1-\omega) + \omega CO + \frac{\omega}{2} O_2$$

and

$$r_{CO} = \frac{\omega}{1 + \frac{\omega}{2}}$$

$$r_{O_2} = \frac{\frac{\omega}{2}}{1 + \frac{\omega}{2}}$$

$$r_{CO_2} = \frac{1 - \omega}{1 + \omega/2}$$

Therefore

$$K_c = \frac{\left(\frac{\omega}{1 + \omega/2}\right)^2 \left(\frac{\omega/2}{1 + \omega/2}\right)}{\left(\frac{1 - \omega}{1 + \omega/2}\right)^2} \frac{P}{RT}$$

$$= \frac{\omega^3}{2(1 - \omega)^2(1 + \omega/2)} \frac{P}{RT}$$

From which ω can be calculated, knowing K_c, for a particular temperature. If we allow y excess air in the combustion equation, the relationship becomes

$$K_c = \frac{\omega^2(\omega/2 + \frac{5y}{3})}{(1 - \omega)^2(1 + \omega/2 + \frac{5y}{3})} \; \frac{P}{RT}$$

The combustion reaction is then written

$$C_3H_8 + 5(1 + y)O_2 + 18.8\ (1 + y)N_2 = 3CO_2(1 - \omega) + 3\omega\ CO + (3/2\omega + 5y)O_2$$

$$+ 4H_2O + 18.8\ (1 + y)N_2 \qquad (1)$$

In order to determine the temperature and the degree of dissociation of the combustion products for a particular amount of excess air, it is necessary to provide another relationship between these parameters, and the heat balance for the reaction does just this.

Writing the heat balance for the reaction

$$h_{pr} + h_{O_2}\ 5(1 + y) + 18.8\ (1 + y)\ h_{N_2}$$

$$= 3\ (h + h_t - h_{537})_{CO_2}\ (1 - \omega) + 3(h + h_t - h_{537})_{CO}(\omega)$$

$$+ 4(h + h_t - h_{537})_{H_2O} \qquad (2)$$

$$+ (\tfrac{3}{2}\omega + 5y)(h + h_t - h_{537})_{O_2}$$

$$+ 18.8\ (1 + y)\ h + h_t - h_{537})_{N_2}$$

where

h is the heat of formation

h_t is the enthalpy at temperature t

h_{537} is the enthalpy at the datum level of 77°F

From Van Wylen (23)

$h_{O_2} = h_{N_2} = 0.0$ $\qquad h_{537CO_2} = 4030.2$ Btu/lb mole

$h_{C_3H_8} = -44{,}676$ Btu/lb mole $\qquad h_{537CO_2} = 3729.5$ Btu/lb mole

$h_{CO_2} = -169{,}293$ Btu/lb mole $\qquad h_{537H_2O} = 4268.2$ Btu/lb mole

$h_{CO} = -47{,}548$ Btu/lb mole $\qquad h_{537O_2} = 3725.1$ Btu/lb mole

$h_{H_2O} = -104{,}071$ Btu/lb mole $\qquad h_{537N_2} = 3729.5$ Btu/lb mole

This gives

$$979{,}448.6 + 79{,}423.1y - 3h_{tCO_2} - 4h_{tH_2O} - 5yh_{tO_2} - 18.8\,(1+y)h_{tN_2}$$

$$= 320{,}549.5\omega + 3\omega\left(h_{tCO_2} - h_{tCO} + \frac{h_{tO_2}}{2}\right) \qquad \text{(2a)}$$

A value of excess air, y, is chosen, and the variation of adiabatic combustion temperature with degree of dissociation is found for equation (1) and (2) respectively. The results are plotted on the same graph, as in Figure 13, and the point of intersection of the two curves gives the condition of the combustion reaction for that value of excess air.

The drop in flame temperature due to dissociation is shown in Figures (14) and (15). It will be seen in Figure (14), where the flame temperature is plotted against the fraction of the theoretical fuel required for stoichiometric combustion, f, ($= \frac{1}{1 + y}$), that as pointed out earlier, the simple analysis gives a reasonable approximation for lean mixtures, but is relatively inaccurate at higher temperatures. Figure (15) shows a decrease in flame temperature of 200°R for no excess air, and this value compares well with those quoted by Schmidt (22) in the following table

Fuel		Combustion Temperature		Drop in Temperature
		Without Dissociation	With Dissociation	
Petrol	f = 1.2	4664°R	4435°R	229°R
	f = 0.8	4757°R	4604°R	153°R

where f is the fraction of theoretical fuel.

The calculation of the adiabatic combustion temperature for a more sophisticated fuel is more complicated than the method described here, chiefly because it is necessary to satisfy several equilibrium conditions simultaneously. Besides the dissociation of carbon dioxide, water vapour splits into hydrogen and hydroxyl ions hydrogen and oxygen dissociate, and many other minor reactions take place. A numerical solution would be arrived at by considering the mass conservation of the components, the chemical reaction equation and the equilibrium of the reaction. As pointed out earlier, no other reaction has been considered other than the dissociation of carbon dioxide.

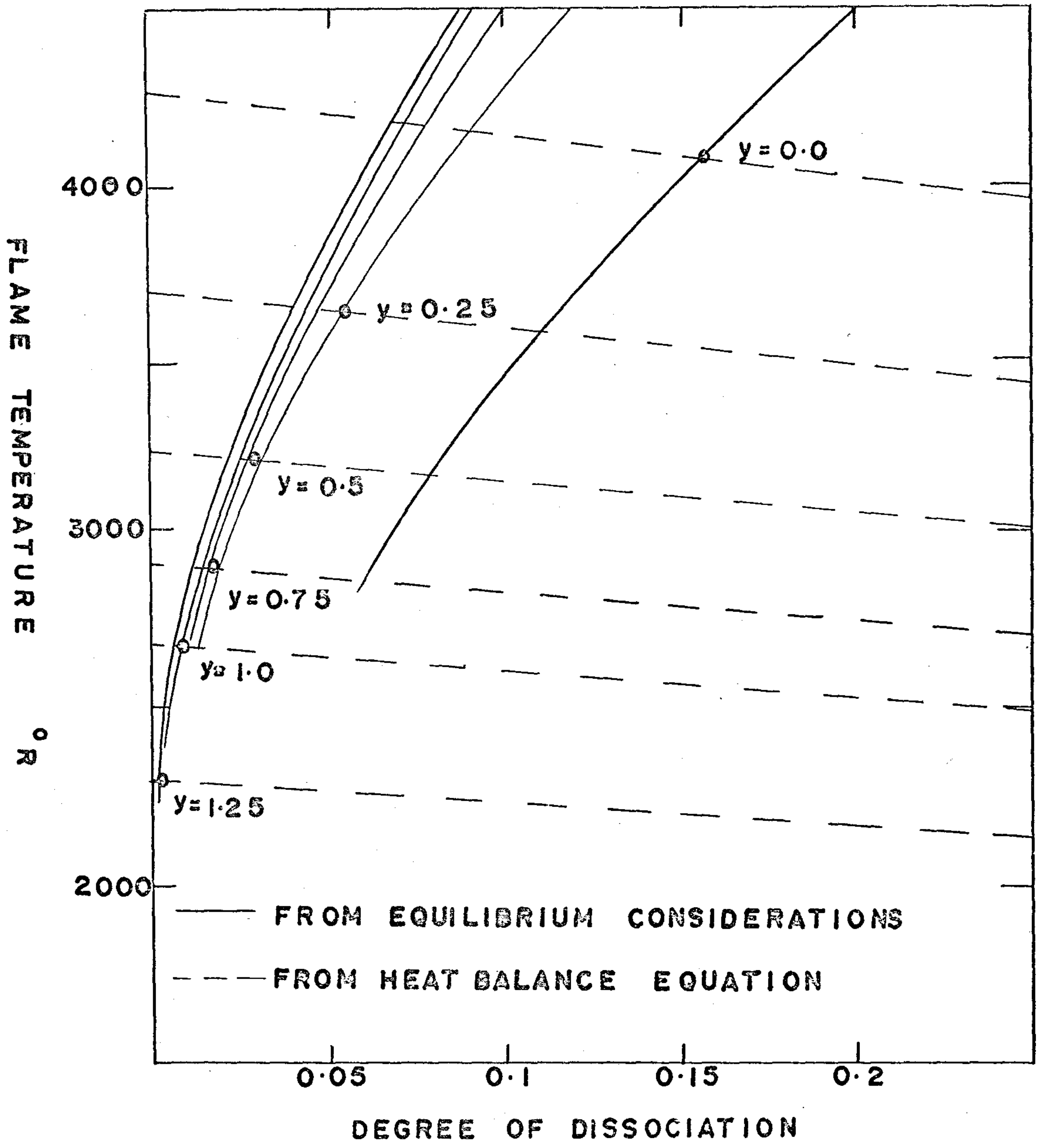

FIGURE 13

Adiabatic Flame Temperature vs

Degree of Dissociation of Carbon Dioxide

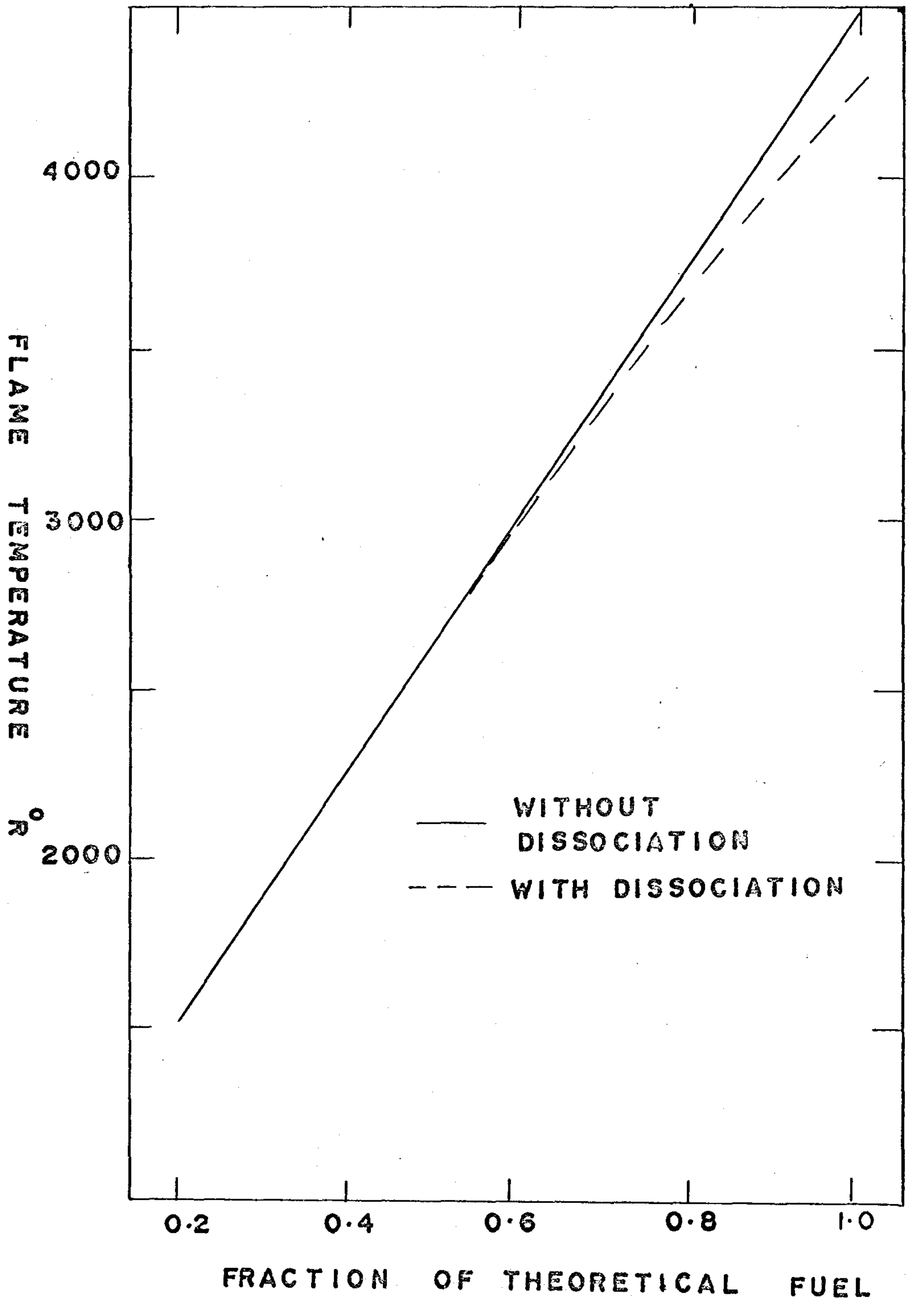

FIGURE 14

Adiabatic Flame Temperature vs Fraction of

Theoretical Fuel for the Stoichiometric Combustion of Propane

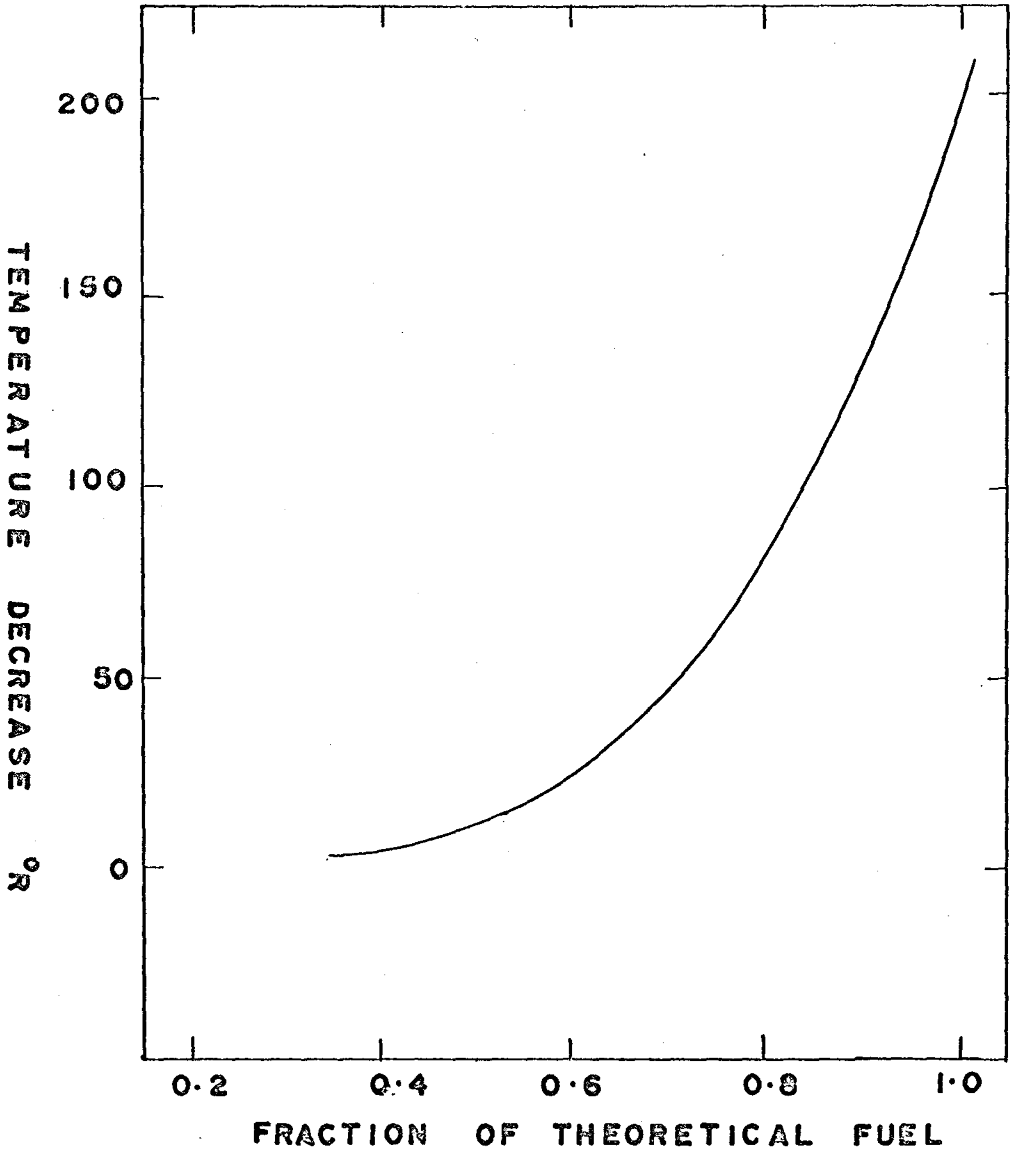

FIGURE 15

Flame Temperature Decrease due to the Dissociation of Carbon Dioxide vs Fraction of Theoretical Fuel for the Stoichiometric Combustion of Propane

5. DESCRIPTION OF APPARATUS

5.1 Combustion Section

The combustion section of the apparatus consists of a flame tube which is enclosed in an outer casing, see Figure 16. The air is led into the combustion chamber through the plenum chamber from the downstream end, and is distributed evenly round the circumference of the flame tube by the twelve holes, each 5/8 inch in diameter, drilled 3/4 inches from the downstream end. This counterflow of air serves to cool the flame tube, and provides the secondary flow of dilution air, as well as the air used for combustion. The outer casing is made from 4 inch nominal bore pipe, and is 10-3/8 inches long. The plenum chamber is a 2 inch wide, 6 inch nominal bore pipe, bounded by and welded to two stainless steel plates, both of which are welded to the outer casing. The one plate at the downstream end, has an inner diameter diameter of 3-1/4 inches, and serves to locate the flame tube. Two windows were placed in the outer casing, in order to be able to inspect the flame tube during a test run. The glass, Vycor #7913, was supplied by Canadian Pittsburgh Industries Limited.

The flame tube, Figure 17, is made from Hastelloy Alloy X, whose properties are listed in Appendix I, and is 3 inches in diameter and 10 inches in total length. It is supported by the air swirler at one end, and by two short legs at the downstream end. A lip on the flame tube fits snugly up to the plate at the downstream end and by virtue of the thermal expansion and internal pressure is held securely in position, thus preventing any air leakage. The ignition spark plug is welded into the body of the flame tube, and the secondary dilution air flows through three rows of eight holes, each 7/32 inches in diameter.

The propane gas is led through the casing end plate to the primary zone of the flame tube by a 5/16 inch tube. The air swirler is held in position round the tube , by the gas nozzle, which screws into the tube and has six 1/64 inch holes through which the propane enters the mixing area. The swirler gives a rotation to the incoming air, thereby improving mixing, and combustion.

A ten inch long section of 4 inch nominal bore pipe is provided downstream of the combustion section. This contains the combustion gases, so that temperature and pressure measurements could be made. Four ceramic inserts were put in the wall, through which the pressure probe and the thermocouple were inserted. This section leads the gases to a large exhaust section, which takes the gases to atmosphere, and provides for a glass window, so that a view may be had to the primary zone of the flame tube. The air swirler and nozzle are shown in Figures 18 and 32

5.2 Air and Propane Supply

The supply lines for the apparatus are shown in Figure (19). In order to obtain gaseous propane, since the vapour pressure at normal temperatures and pressures is of the order of 125 p.s.i.a., it is necessary to pump the liquid propane to a vapouriser, where the propane is heated, and delivered to the combustor at the required pressure. Any excess liquid propane is fed back to the tank through a bypass valve. A solenoid valve, controlled from the central control panel, allows flow to the system, and after shutdown, another valve clears the pipeline of the propane left in it. The flow of propane is metered by a previously calibrated rotameter. The air is taken from a compressor at approximately 80 p.s.i., and after being filtered, and passed through a dryer * to remove any moisture, is led to the plenum chamber. The flow is metered using a rotameter, which had been previously calibrated.

5.3. Control

The control of the propane flow is accomplished electrically, while the air flow is adjusted manually. After the required air flow is obtained, the propane pump is activated. At the same time a solenoid valve, normally closed is opened to allow flow to the combustion chamber. The solenoid valve that is normally open to allow the propane to clear from the supply line, is also closed. Ignition of the combustible mixture is obtained by use of a momentary contact switch, which energizes a transformer, whose secondary side delivers six thousand volts to the ignition spark plug. At the same time a fan is started in order to clear the working area of any combustion products.

* Lectrodryer Type BAC-90

After the required tests have been made, the power from the mains is switched off, and the pump ceases to deliver propane. The solenoid valve, allowing flow to the system, closes and the other solenoid valve opens to clear the line of propane gas. The electrical wiring diagram is shown in Figure (20).

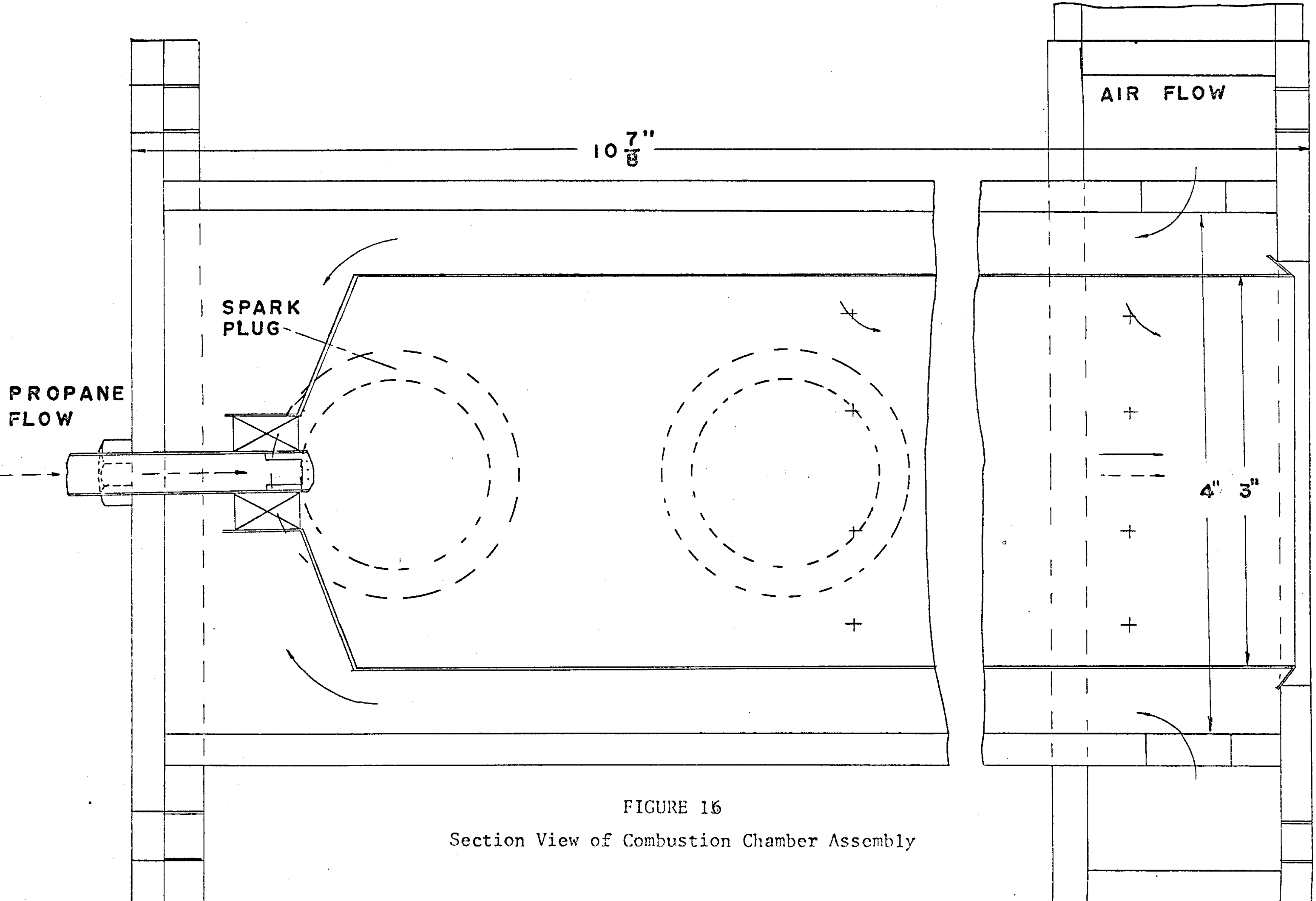

FIGURE 16

Section View of Combustion Chamber Assembly

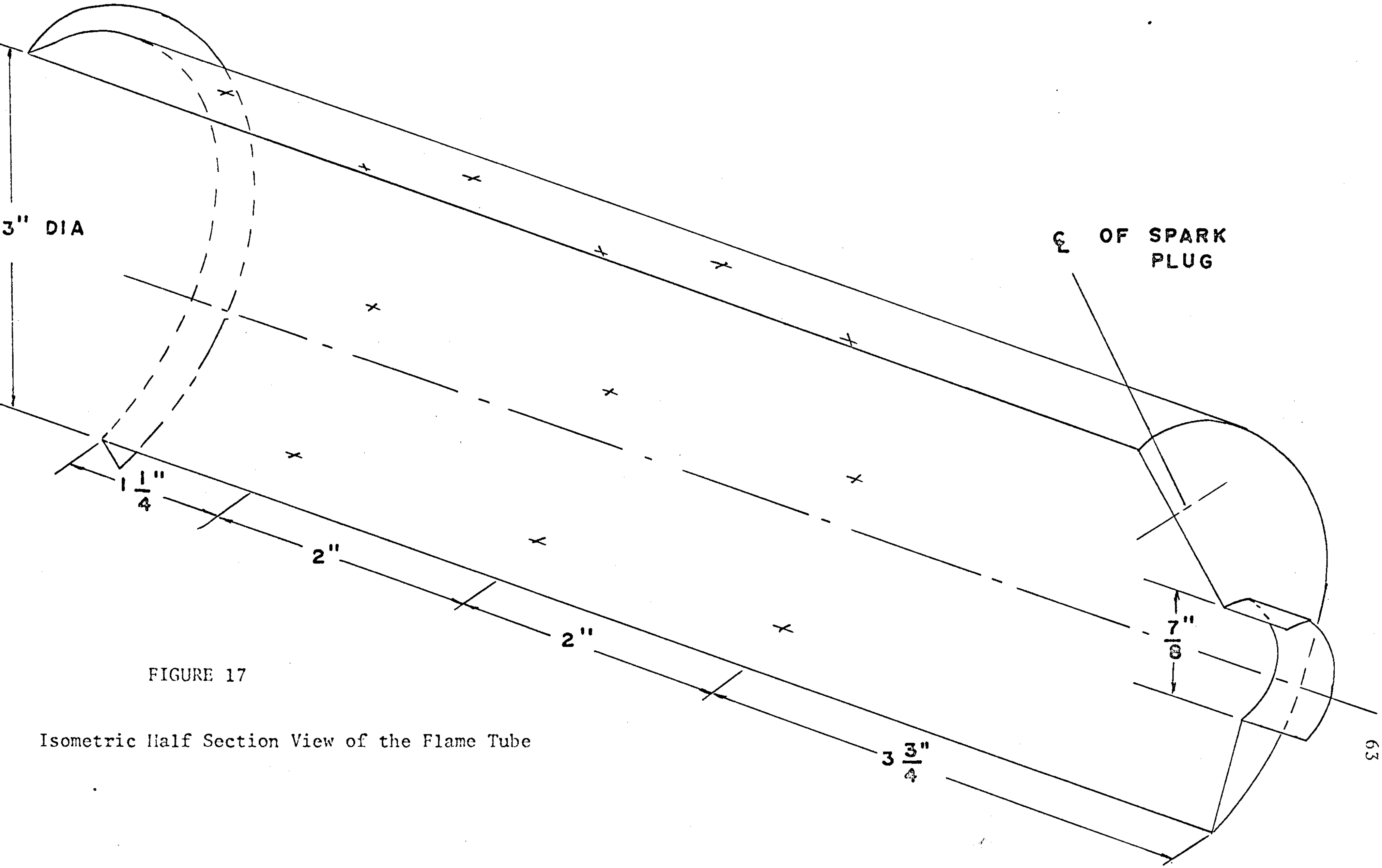

FIGURE 17

Isometric Half Section View of the Flame Tube

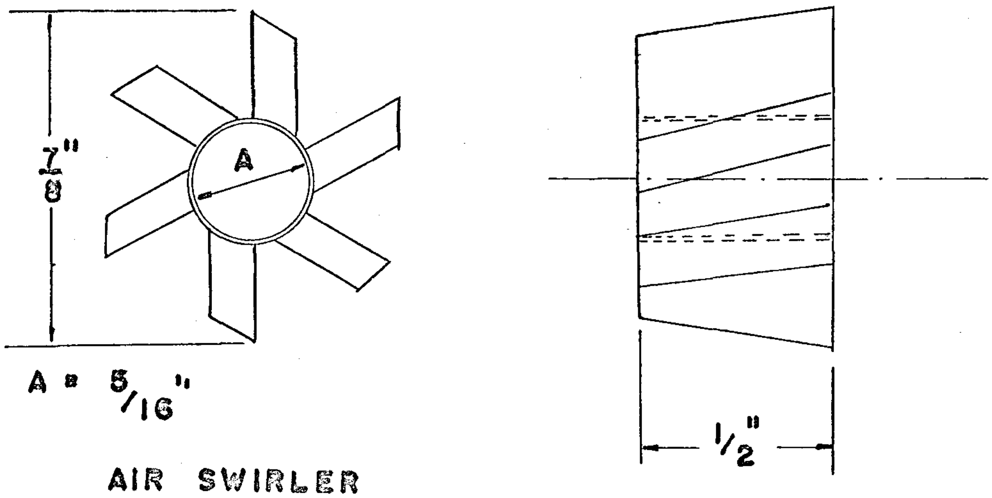

AIR SWIRLER

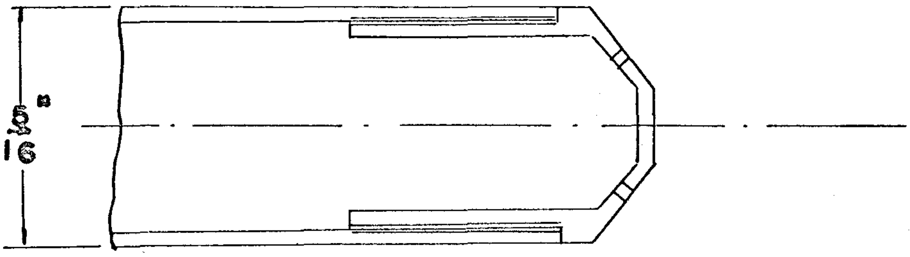

GAS NOZZLE

FIGURE 18

The Air Swirler and Gas Nozzle

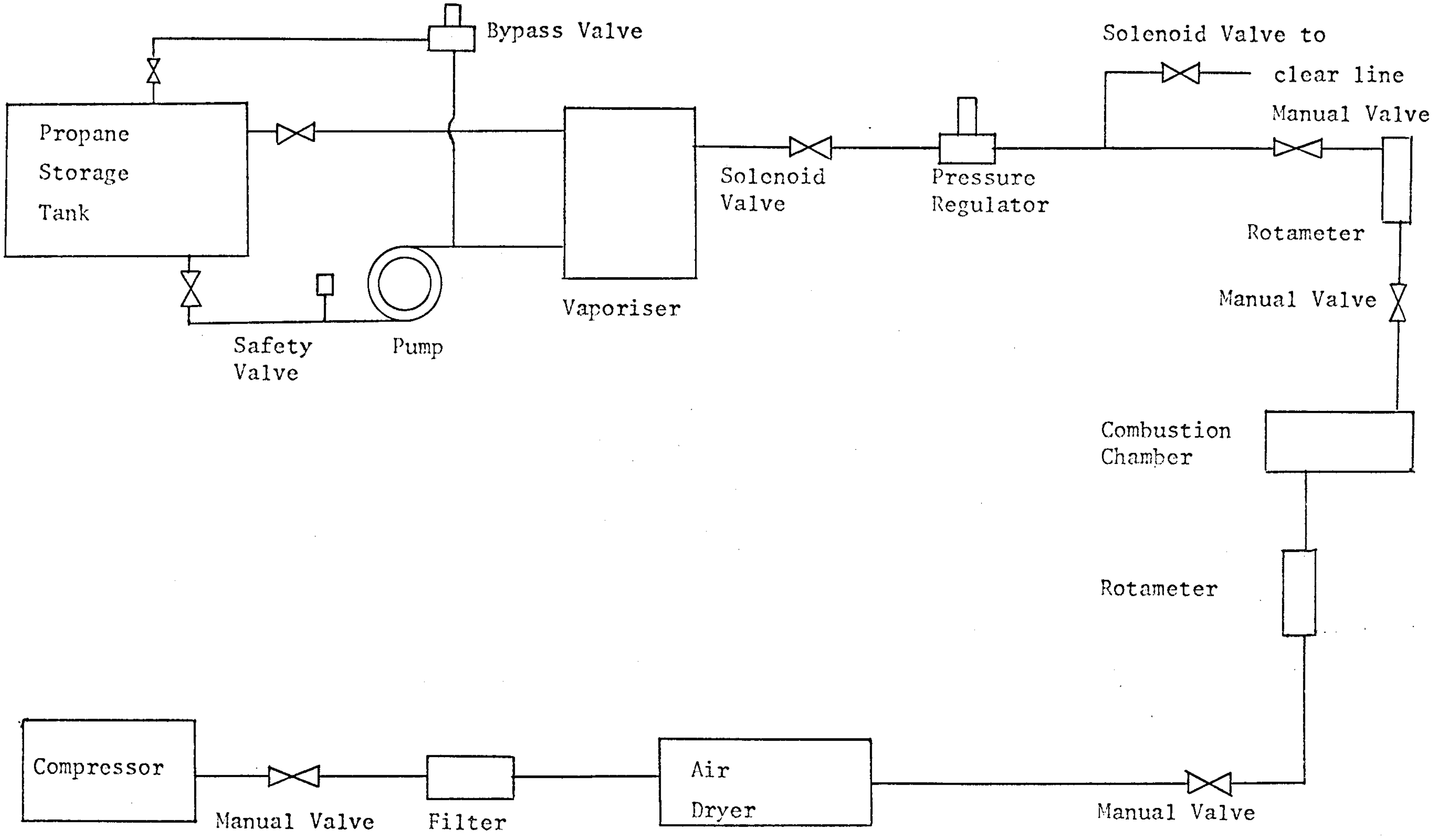

FIGURE 19

Schematic of Air and Propane Supply Lines

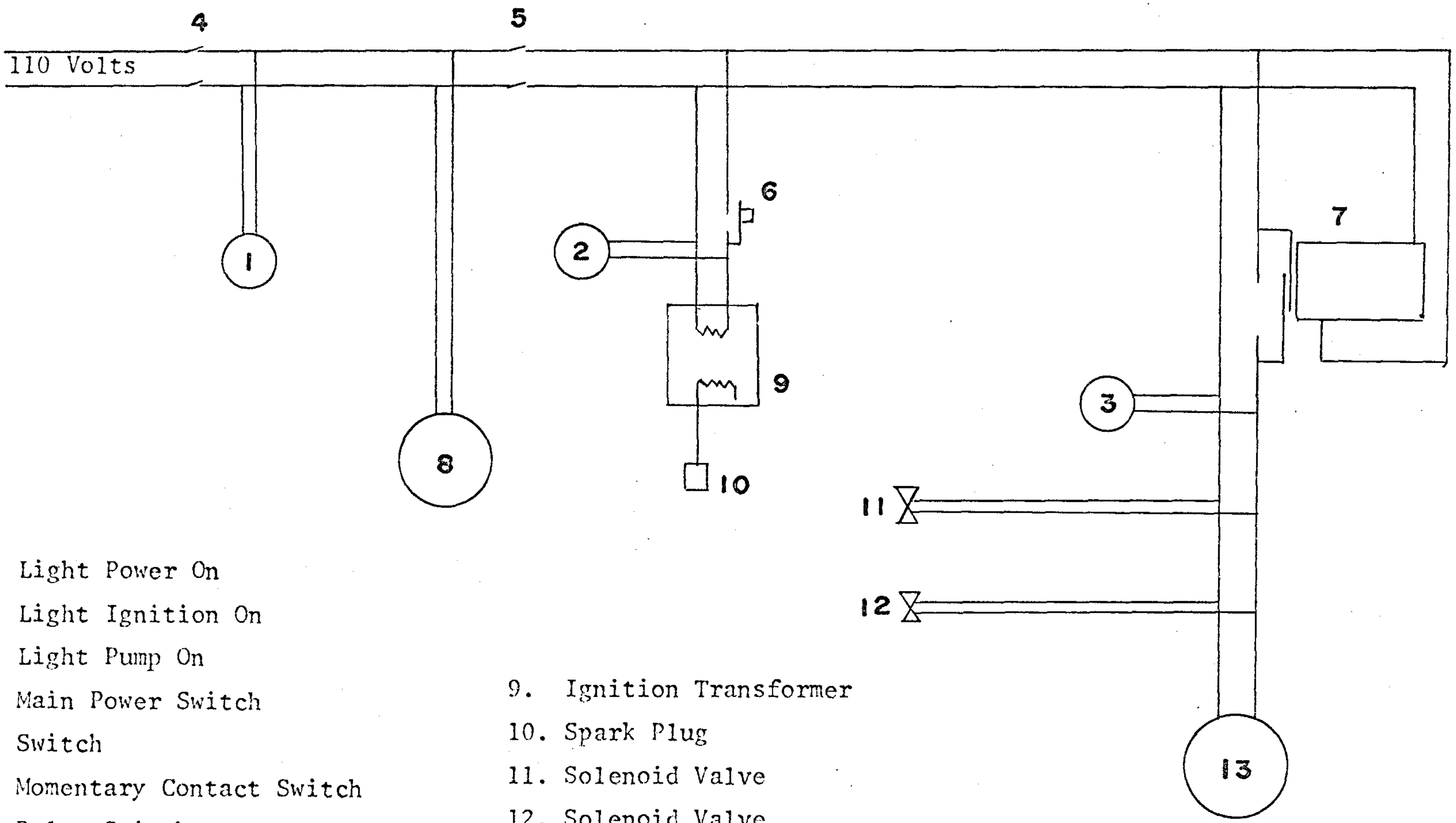

1. Light Power On
2. Light Ignition On
3. Light Pump On
4. Main Power Switch
5. Switch
6. Momentary Contact Switch
7. Relay Switch
8. Fan
9. Ignition Transformer
10. Spark Plug
11. Solenoid Valve
12. Solenoid Valve
13. Propane Pump

FIGURE 20

Schematic of Electrical Wiring

6. DISCUSSION OF EXPERIMENTAL PROCEDURE AND RESULTS

6.1 Temperature Measurement

In order to compare the performance of the combustion chamber with the theoretical results obtained in Section 4, it is necessary to measure the flame temperature in the primary zone. The difficulty is to be sure exactly what a representative value of the flame temperature is. The flame varies in intensity due to the variation in concentration of fuel in the primary zone, brought about by the uneven injection of fuel from the gas jets, and the flame temperature will vary accordingly. A platinum-10% rhodium/platinum thermocouple junction was inserted into the flame tube and placed one inch in front of the gas nozzle, around which it could be rotated taking random readings of temperature. It was thought that this procedure would give the most representative value of flame temperature. The thermoelectric potential, with reference to a distilled water ice bath, was measured with a potentiometer*, and the millivolt-temperature conversion was done using the National Bureau of Standards values.

Six chromel-alumel thermocouple junctions were attached to the body of the flame tube in order to determine the mean temperature of the metal. Three thermocouples were placed symmetrically round the circumference between gas nozzle and the

---

* Rubicon Portable Precision Potentiometer Type No. 2745

first row of dilution holes, and the other three, in similar circumferential positions halfway between the first and second set of dilution air holes. These thermocouple positions are shown in Figure 26. The thermoelectric potential was again measured using the precision potentiometer.

The temperature of the combustion gases in the exit plane of the flame tube, was measured using a platinum-10% rhodium/platinum thermocouple junction. A traverse was made across the diameter of the flame tube in order to ascertain whether the mixing in the primary and dilution zones was at all effective.

6.2 Pressure Measurement

The stagnation pressure of the exhaust gas stream was measured at a position just downstream of the exit plane of the flame tube, using a probe made from 1/16" ID Inconel alloy tubing.

In order to calculate the air fuel ratio, the pressure of the air and the propane as they pass through the rotameters must be known. Pressure tappings were made downstream of the rotameters, and the pressure was measured using two precision dial manometer capsule type gauges*.

The barometric pressure was measured with a temperature corrected mercurial barometer**.

* Wallace and Tiernan Precision Dial Manometers, Type FA-145

** Wallace and Tiernan Precision Mercurial Manometer Type FA-135

6.3 Measurement of Air-Fuel Ratio

The instantaneous flow rate of air and propane is measured by two rotameters*. These were calibrated at a certain temperature and pressure, and a correction must be made for the actual temperature and pressure of the fluid, whose flow rate is to be measured. The rotameters are calibrated in terms of the equivalent air flow, V_{eq}, at 14.7 p.s.i.a. and 70°F, for a specified temperature, pressure, and fluid specific gravity (Condition 1). If the rotameter is used at a temperature, pressure and specific gravity (Condition 2), other than the original specifications, a correction factor must be applied.

$$\text{The correction factor} = \sqrt{\frac{Sg_i \; T_i \; p_2}{Sg_2 \; T_2 \; p_1}}$$

where T is the absolute temperature p = p.s.i.a

Sg = the specific gravity, which for air is 1.0

This then gives the equivalent air flow for the operating conditions 2. To convert this to metered gas flow, we use the following relationship, given in Brooks Technical Bulletin T-022, Guide to Rotameter Application.

$$V_{eq} = \frac{M \left(\frac{53.3 \times 530}{14.7 \times 144}\right)}{Sg_2} \sqrt{\frac{Sg_2 \times T_2 \times 14.7}{1.0 \times 530 \times p_2}}$$

---

* 1) Air-Brooks AR-MET Rotameter Model 1118 with Magnetic Follower Indicating Extension.

* 2) Propane-Brooks Full View Glass Tube Rotameter Model 1110

where Sg is the specific gravity of the fluid, and M is the mass flow rate in lbs/min of the fluid considered.

Hence

$$M = \frac{V_{eq} \; Sg_2}{13.34\sqrt{\frac{Sg_2}{1.0} \; \frac{T_2}{530} \; \frac{14.7}{p_2}}}$$

$$V_{eq} = V_c\sqrt{\frac{Sg_1}{Sg_2} \cdot \frac{T_1}{T_2} \cdot \frac{p_2}{p_1}}$$

where V_c is the calibrated flow reading.

For the propane rotameter

T_1 = 530°F

p_1 = 140 p.s. i. g.

$Sg_1 = Sg_2 = 1.56$

Therefore

$$M_p = \frac{V_{cp}\sqrt{\frac{p_{2p}}{140 + p_o}} \; (1.56)}{13.34\sqrt{\frac{1.56}{1.0} \cdot \frac{T_{2p}}{530} \cdot \frac{14.7}{p_{2p}}}}$$

Similarly for the air flow, $Sg_1 = Sg_2 = 1.0$ and $p_1 = 100$ p.s.i.g.

Therefore

$$M_a = \frac{V_{ca}\sqrt{\frac{p_{2a}}{100 + p_o}} \; (1.0)}{13.34\sqrt{\frac{1.0}{1.0} \cdot \frac{T_{2a}}{530} \cdot \frac{14.7}{p_{2a}}}}$$

Where p_o is atmospheric pressure

The overall air fuel ratio is then

$$\frac{M_a}{M_p} = \frac{1}{1.56} \cdot \frac{V_{ca}}{V_{cp}} \cdot \frac{p_{2a}}{p_{2p}} \sqrt{\frac{T_{2a}}{T_{2p}}} \sqrt{\frac{(140 + P_o)(1.56)}{100 + P_o}}$$

In order to determine what proportion of the air is used in combustion, and what part for dilution, three tappings were made in the outer casing, and through which a pitot static probe could be inserted into the annulus, between the dilution holes and the air swirler, in order to determine the dynamic head, and hence the mass flow of air to the combustion zone. The results obtained point to the fact that the air flow is not evenly distributed in the annulus, and because of this no estimate could be made by this method of the air entering the combustion zone. The position of the pressure tappings is shown in the sketch below, and the results obtained are further discussed in Section 7.

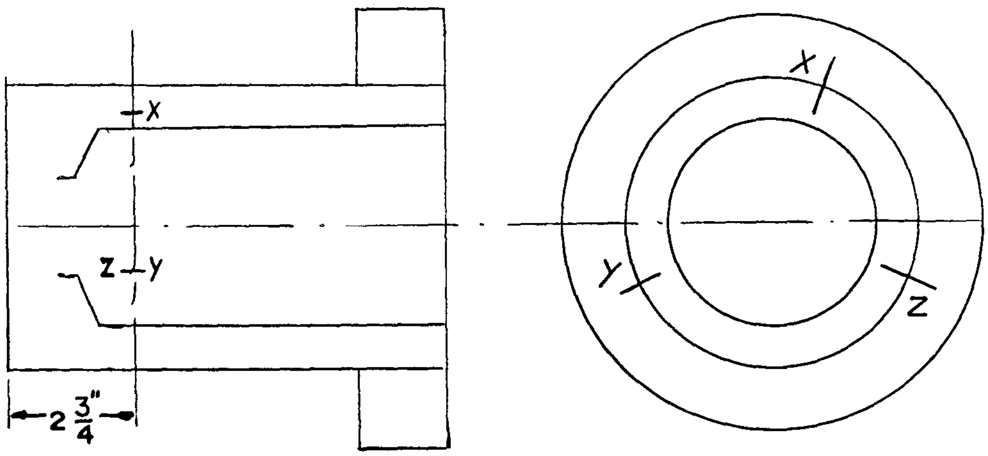

Two static pressure taps each 0.03 in. dia. were made in the flame tube, where the air flows through the air swirler. The total pressure of the flow was measured in the annulus of the combustion chamber, and using the assumption that the total pressure remains constant, the dynamic head can then be measured. The difference in value of the static pressures was of the order of 0.3 in of water, and the mean value was used. Knowing the temperature of the air, and the area of the swirler, the air mass flow to the primary zone could then be calculated, and hence the fraction of the total air flow used for combustion is then known. The air velocity for the maximum flow was of the order of 250 ft/sec.

The following readings were taken

M_a lbs/sec	M lbs/sec	M/M_a
0.113	0.0744	0.66
0.098	0.065	0.66
0.084	0.054	0.65
0.064	0.042	0.66
0.073	0.049	0.67
0.092	0.060	0.65

where M_a is the total air flow.

M is the air flow to the primary zone.

and hence $\frac{M}{M_a}$ is the fraction of the total air flow that is used for combustion. An average value of 0.66 was used, and the air fuel ratio in the primary zone is then

$$Z = \frac{0.66}{1.56} \frac{V_{ca}}{V_{cp}} \frac{p_{2a}}{p_{2p}} \sqrt{\frac{T_{2a}}{T_{2p}}} \sqrt{\frac{(140 + p_o)(1.56)}{100 + p_o}}$$

This value is used in the presentation of the results.

When rich mixtures were used it was noticed that the combustion of unburnt fuel took place in the dilution air jets. A value of fuel flow was set, and the air flow was increased, until the burning in the jets just ceased. The overall air-fuel ratio at this point was 22.4. Assuming that the air fuel ratio in the primary zone was that required for stoichiometric combustion, i.e. 15.72, the fraction of the total air flow reaching the combustion zone, is then $\frac{15.72}{22.4} = 0.7$, which corresponds to that value arrived at by measurement and calculation.

6.4 Miscellaneous Observations

It was noted in Section 3.1 that the limits of flammability for any fuel lie between the approximate values of air-fuel ratio of 8 and 30, whereas the stiochiometric value is in the order of 15. Although ignition of the combustion mixture did not take place until an air-fuel ratio of about 22 had been reached, due to local conditions in the combustion zone, once ignition had taken place, it was possible to reduce the flow of fuel to an air fuel ratio of 30.5, when extinction of the flame took place. No such extinction could be obtained when rich mixtures were used.

The dilution air holes were designed to give penetration to the centre line of the flame tube, but in practice the penetration of the dilution air jet, which could be seen when the combustion of unburnt fuel took place in the jets, was approximately 50% of the intended value. This was probably due to the uneven distribution of air in the annulus, coupled with the fact that the pressure in the annulus was much lower than expected.

It was found that the flow of propane gas was limited to a definite maximum value of 0.007 lbm/sec. This was due to the choking of the gas nozzle, at this flow rate.

6.5 Experimental Results

Three sets of data for the flame temperature were taken using an unshielded thermocouple and are presented in graphical form in Figures 21, 22, 23, and in tabular form in Appendix 2. In order to determine what effect radiation had on this temperature reading, a further set of data were taken using a shielded thermocouple junction, and Figure 24, shows the comparison between the results using the shield, and those obtained without a shield. The sketch below shows the type of shield used.

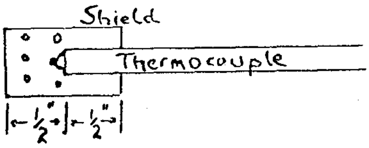

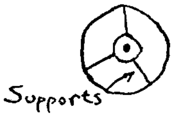

A comparison between the calculated values of flame temperature, and the experimental data are given in Figure 25. The flame temperature is given in each case as a function of the fraction of the theoretical amount of fuel required for stoichiometric combustion.

Only one set of data was taken for the flame tube wall temperature, as it was considered necessary only to ascertain whether the metal temperature remained within the prescribed limits, as required by the physical properties of the alloy. The wall temperatures are presented in Figure 26, and are tabulated in Appendix 2.

The variation of the flame tube exit plane temperature is given for a variety of air fuel ratios in Figures 27, 28, 29. The three sets of data correspond to three positions of the gas nozzle. Data was not taken for the rich mixture range, as it is not intended that the combustion chamber should operate under these conditions. The static pressure of the exhaust gases was considered to be a constant value, as any variation was so small as to be undectable. The dynamic pressure of the gas flow was equal to 0.5 in of water, which for the average temperature measured represents a velocity range of 80 to 120 ft/sec in the flame tube.

The maximum rate of air mass flow as measured by the rotameter was 0.113 lbm/sec. As a check on this value a pitot static probe was inserted into the air line, immediately downstream of the rotameter and a measure made of the dynamic head, the average value of which was found to be 3.2 in of water. The mass flow rate through pipe of diameter 1.5 in. is then calculated to be 0.112 lbm/sec., which agrees well enough with that value provided by the rotameter.

7. DISCUSSION OF EXPERIMENTAL RESULTS

For mixtures which are more lean than an air-fuel ratio of 27.2, which expressed as a fraction of the theoretical air-fuel ratio required for stoichiometric combustion. has a value of 0.6, the flame temperatures obtained agree very well with those predicted by the theoretical calculation. This agrees with the assertion made in Section 4, when discussing the validity of the theoretical analysis. At air-fuel ratios less than this value, the flame temperature obtained falls below that predicted, and the maximum value obtained experimentally, which for the three test runs was 2933°F, 2947°F, and 2968°F respectively, was approximately 1000° lower than that predicted by calculation. This represents a combustion effeciency of 75% at the maximum flame temperature reached, and as such agrees with the value quoted in Section 3.3. The air-fuel ratio at which the maximum temperature was obtained varied from 16.85 to 16.5. The effect of radiation from the flame to the thermocouple, and from the latter to the wall is not very significant, as the comparison between the flame temperatures recorded by a shielded junction, and an unshielded junction, shows. A slightly higher maximum temperature was recorded, at a leaner mixture than before, but the magnitude of this temperature does not differ appreciably in the two cases. Tests 1,2, and 3 were done when the nozzle was in position 1, as per Figure 27, and the data for the radiation effect was taken with the nozzle in position 3, as per Figure 29. It would seem therefore, that the nozzle position makes little or no difference to the average flame temperature.

Temperature profiles were taken in the exit plane of the flame tube, by traversing a thermocouple junction horizontally across the diameter of the tube. The data presented in Figure 27, was taken with nozzle in position 1, and it was first thought that the large temperature variation could be rectified by a slight change in the nozzle position. The nozzle was rotated through 20°, to position 2, and the results obtained are given in Figure 28. It then became obvious that the form of the temperature profile could not be changed by a minor adjustment in nozzle position. Accordingly, the nozzle was rotated through 180° to position 3 and if the temperature variation was due solely to the nozzle, the profile should be reversed. The results obtained, which are given in Figure 29, show that this is not the case. The profile is more uniform, but still exhibits the same tendencies as before, in that the temperature is higher at one side than at the other, although the difference in temperature from one side to the other is reduced from the order of 800° to 300°.

It then became obvious that the air distribution in the dilution zone must be such as to cause unequal cooling and dilution. Three tappings were made in the outer casing, as shown in the sketch in Section 6, and a pitot static tube inserted in order to measure the dynamic head. At position X, no dynamic head could be measured, indicated that a region of still air existed. Positions Y and Z, showed a dynamic head of 0.6, and 0.8 in of water respectively, and that the direction of the air flow was towards the nozzle end, and at an angle 30° below the horizontal. The air flow takes place in the lower part of the annulus between the flame tube and the outer casing, and only a small portion of the flow takes place in the top portion of the chamber. The reason for this is that the air enters the plenum chamber in a downward direction with a velocity in the region of 120 ft/sec., and is thus not able to turn the 90° corner into the upper part of the annulus. Most of the air flows to the lower part of the plenum chamber, and enters the annulus from below, or entering the annulus from above, flows round the flame tube to the lower part. The two air streams meet, and then flow in the lower annulus, and only a small portion flows into the upper part, which remains an essentially stagnated region.

This air distribution causes both uneven cooling of the flame tube, and uneven dilution jet penetration. This is shown in the variation of flame tube wall temperature. Position 3, as designated in Figure 26, corresponds to pressure tapping Y, and position 1, to pressure tapping Z. Position 3 has the hottest temperature, as this is a result of the lack of cooling provided by the air in the annulus, and the temperature distribution in the flame tube, which will be of the same order as in the exit plane.

The high side of the flame tube temperature profile corresponds to position 3. It may also be possible that the flow in the plenum chamber has a preferred direction, thus accounting for the lower temperature of position 1, which corresponds to the colder side of the exit temperature profile.

The non-uniformity of the flame tube exit plane temperature profile and the variation in flame tube wall temperature are due to a combination of air flow distribution in the annulus, and the unequal injection of fuel into the primary zone.

8. DISCUSSION OF THE ERRORS IN THE EXPERIMENTAL WORK

8.1 Errors Associated with the Flame Tube Temperature Measurement

The error involved here is largely due to the uncertainty of an uncalibrated thermocouple. The hot junction was buried in the flame tube wall, by insertion into a 0.02" hole drilled in the metal, and was sealed in by a synthetic porcelain mixture, and consequently it is assumed that the temperature of the metal is that of the junction. The temperature of the cold junction was considered to be in error of ± 0.2°F. The millivolt potential could be measured to ± 0.002 millivolts, which corresponds to 0.1°F. In the range of temperature 530°F to 2300°F, the manufacturers limits of error are ± 0.75%, which for the maximum temperature measured corresponds to ± 13.5 °F.

Two chromel-alumel thermocouple junctions with manufacturers tolerance of ± 0.75% per junction	± 27°F
Cold junction temperature	± 0.2°F
Potentiometer error	± 0.1°F
Total Error	±27.3°F

8.2 Error Associated with the Flame Temperature, and Exit Plane Temperature Measurement

The error involved in the measurement of the hot junction is composed of the same constituents as above. The absolute error for the maximum temperature measured is ± 22°F, and the total error in the measurement is then ± 44.3°F. The question as to whether this measured temperature can be taken as the actual flame temperature is somewhat difficult to answer. As mentioned before the flame temperature will vary according to the local air-fuel ratio, and so the hot temperature junction was moved in a radius of approximately 0.75 in, round the gas nozzle, and several readings were taken at random. The average of these was taken as the flame temperature, and as such no error can be assigned to this measurement.

The error involved in the measurement of the exit plane temperature is again computed from the same considerations as above and the total error is ± 23.8°F.

8.3 Error Associated with the Air-Fuel Ratio Calculation

The accuracy of both the rotameters used is given by the manufacturers as ± 2.0% on the full scale reading. The reading error is ± 0.5% on the full scale reading, so that the total percentage error in the flow rate is ± 2.5%. The error in reading the dial manometers is ± 1.0% on the maximum pressure recorded, and the error present in the manometer itself is ± 2.0% on the maximum pressure, and hence the total possible error is ±3.0%. The error in the measurement of the atmospheric pressure is negligible, as the manufacturers states that the mercurial barometer is accurate to 1 part in 3000. The error in the temperature measurement was ± 0.7% on the readings taken.

Error in measuring flow rate ratio	± 5.0%
Error in pressure ratio	± 6.0%
Error in temperature ratio	± 0.7%
Total error possible	±11.7%

8.4 Error Involved in the Total Pressure Measurement

It is stated in Aerodynamic Measurements (24) that the assumption of isentropic compression at the tip of a probe leads to an error of less than ± 0.2% of the dynamic head, for velocities up to Mach 1. The error due to misalignment of the probe with respect to the flow direction would be of the order ± 0.5% of the dynamic head, for a misalignment of 10° or less.

Assumption of isentropic compression	± 0.2%
Alignment error	± 0.5%
Total error	± 0.7%

This probe error of ± 0.7% of the dynamic head represents ± 0.0035 in water. The reading error on the manometer scale was ± 0.05 in water.

Reading error	± 0.05 in water
Probe error	± 0.0035 in water
Total error	± 0.0535 in water

9. CONCLUSIONS

The preliminary results obtained indicate that the combustion chamber, although relatively unsophisticated compared to one used in an aircraft engine, has a performance that, in terms of combustion efficiency related to adiabatic temperature rise, is at least as good as the performance of a commercial model.

However, in order to obtain a uniform temperature in the exhaust gases both the nozzle configuration and the annulus air distribution must be radically altered. The fuel must be injected evenly into the combustion zone, it is probable that an annular type of nozzle would be better, rather than using one with several distinct injection points, where slight differences in hole size would mean large variations in fuel distribution. In order to obtain a uniform distribution of air in the annulus, the effect of the flow velocity of the air through the pipe must be removed. This would mean a larger plenum chamber, with the addition of baffles, so that the chamber could act as a stagnation region, or the provision of a large axial extension of the outer casing, in order to provide uniform distribution of the air flow.

The temperature of the exhaust gases is in the region of 1900°R, and is therefore lower than that required for sufficient ionization, as pointed out in References 2 and 3, for the efficient operation of a magnetohydrodynamic power generator. The temperature could be raised by reducing the amount of dilution air, to somewhat less than its present value. This would have the added advantage of providing more air to cool the metal surrounding the primary combustion zone. The exhaust gases are at atmospheric pressure, and if the combustion gases are to be injected into a vortex chamber, through the type of nozzle used by Trick (1) in his investigation, higher pressures are required.

One problem is the high level of noise encountered during the tests. At lean mixtures the discomfort is not unbearable, but as the air fuel ratio is reduced, the noise level, possibly aggravated by the exhaust ducting acting as a sounding box, becomes intolerable, but no solution is apparent at the present time.

The operation of the gas supply system, was found to be quite satisfactory, although variation in temperature of the gas in the storage tank, would cause the propane delivery pressure to vary by 5 inches of mercury, for a temperature change of 25 - 30°F. During a test run of about one half hour duration, the gas delivery pressure would drop by 1 - 2 inches of mercury.

10. ILLUSTRATIONS

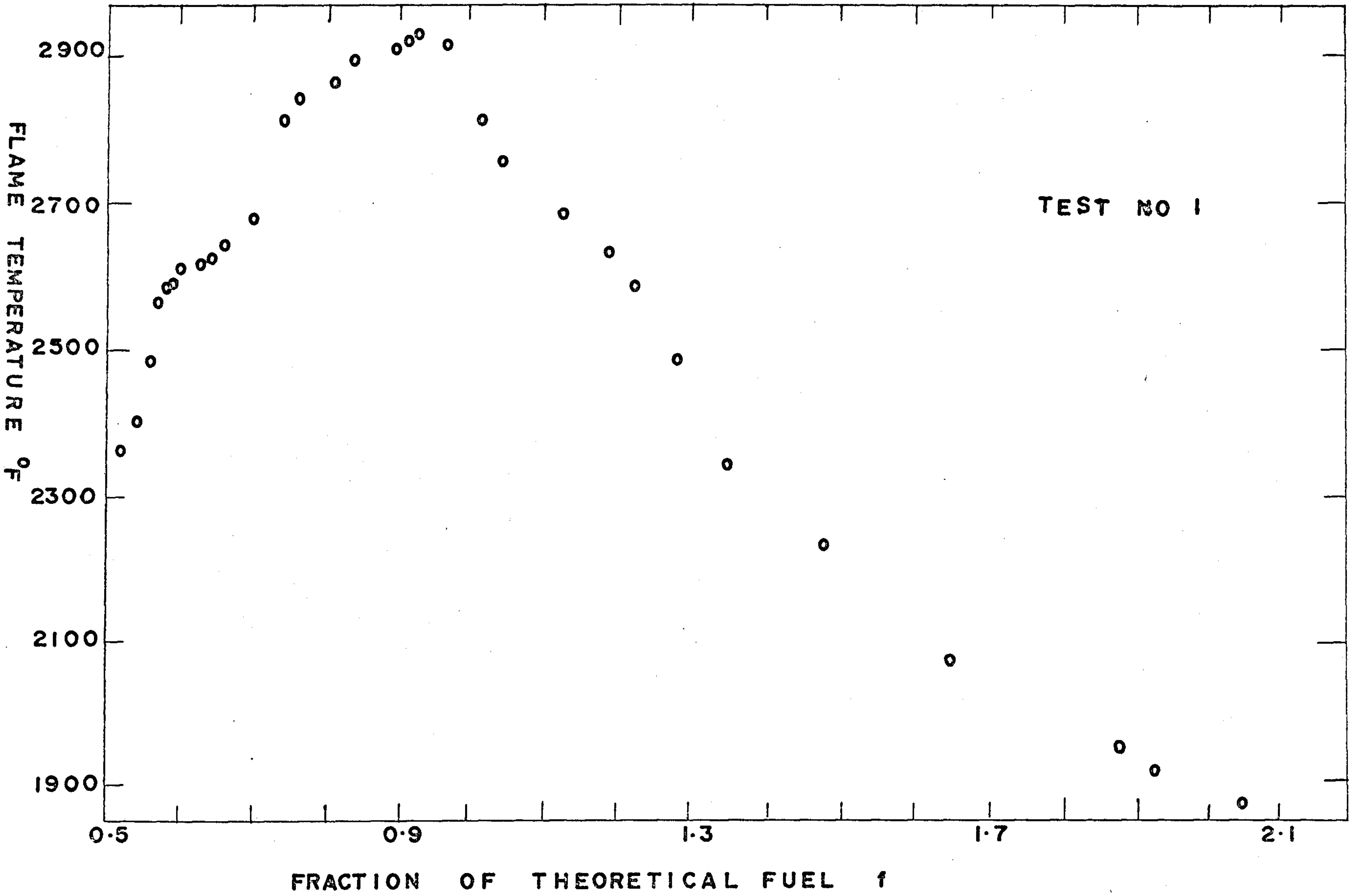

Fig. 21 Experimental Flame Temperature vs Fraction of Theoretical Fuel

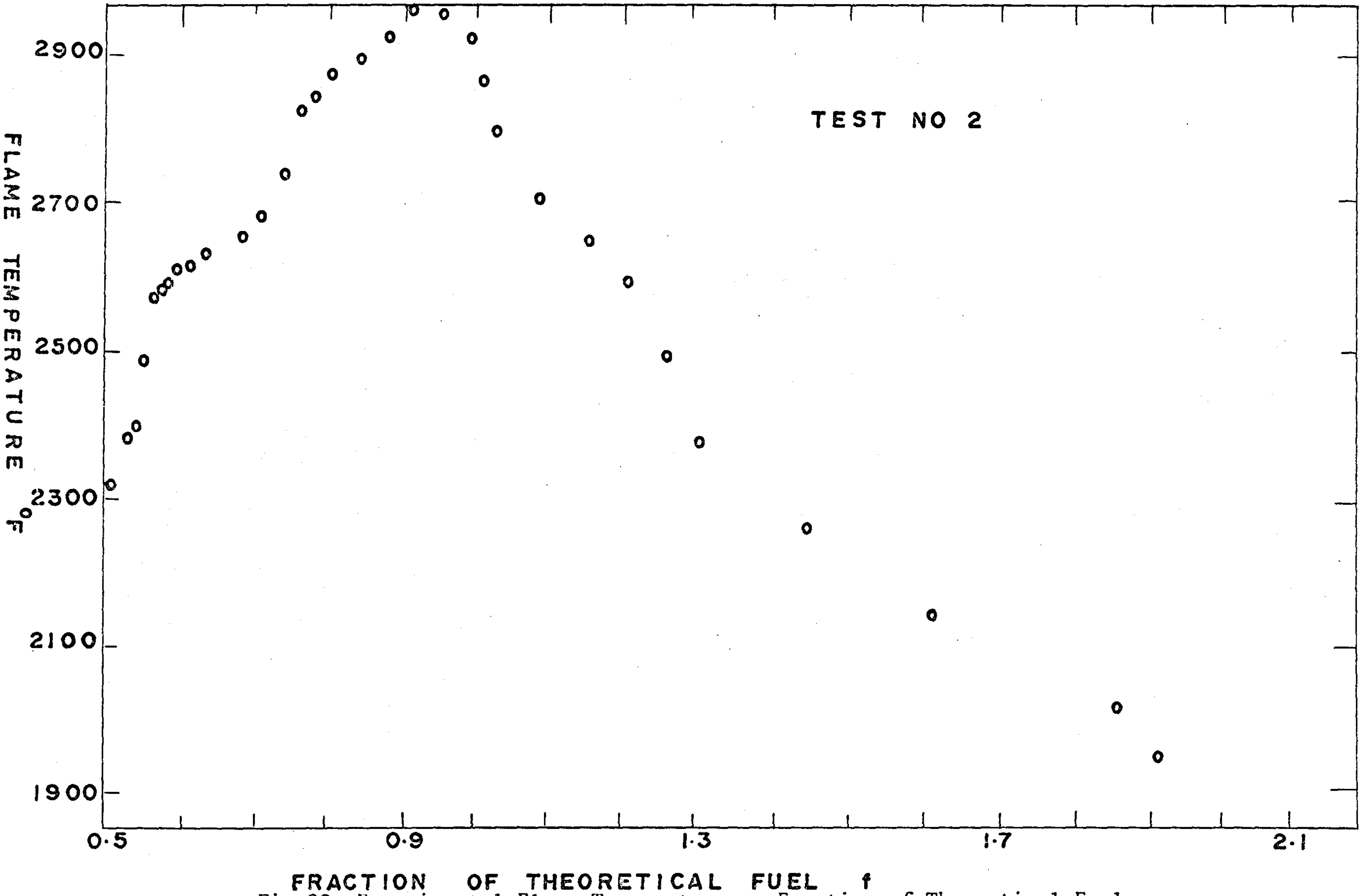

Fig 22. Experimental Flame Temperature vs Fraction of Theoretical Fuel

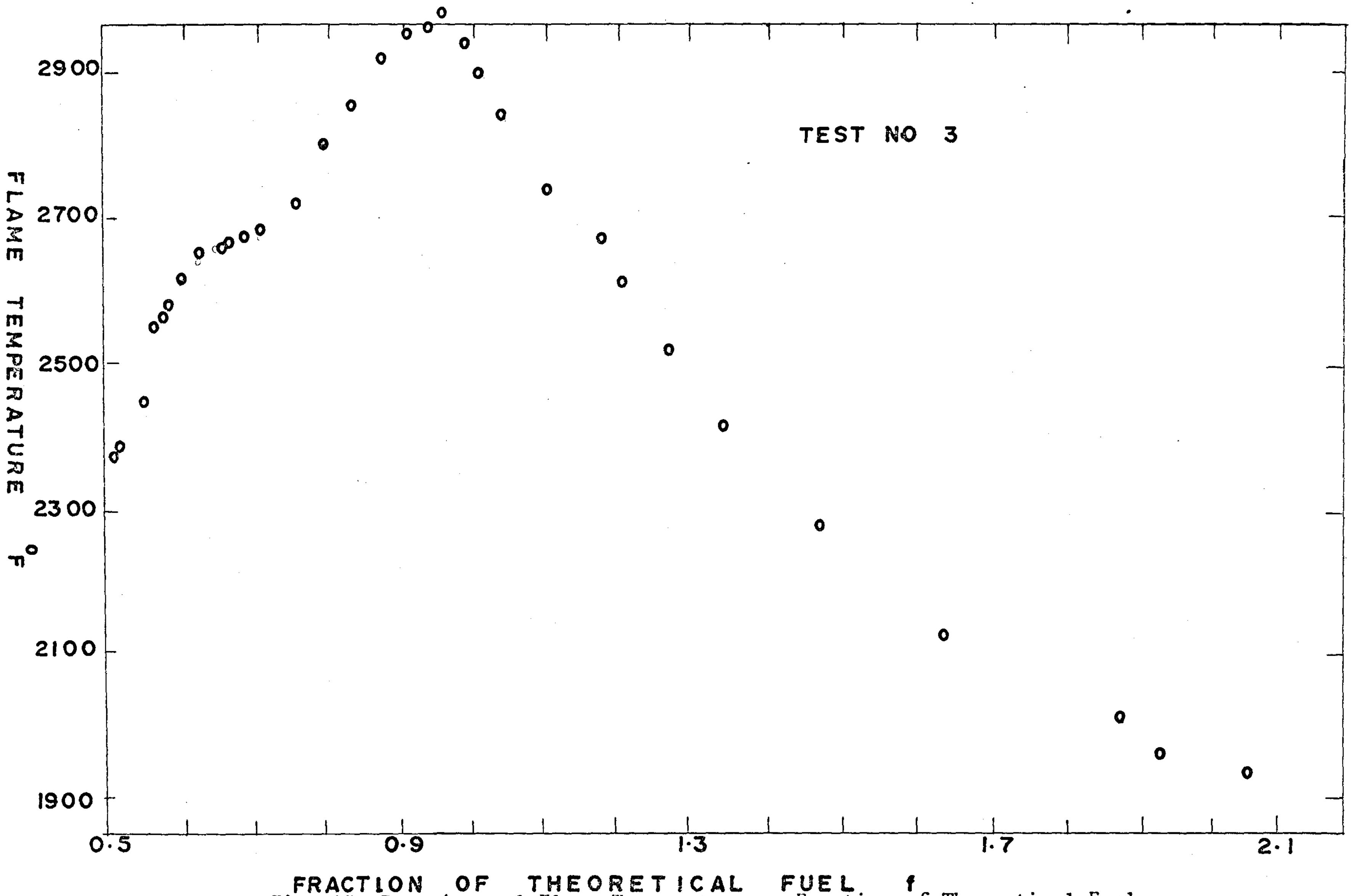

Fig. 23 Experimental Flame Temperature vs Fraction of Theoretical Fuel

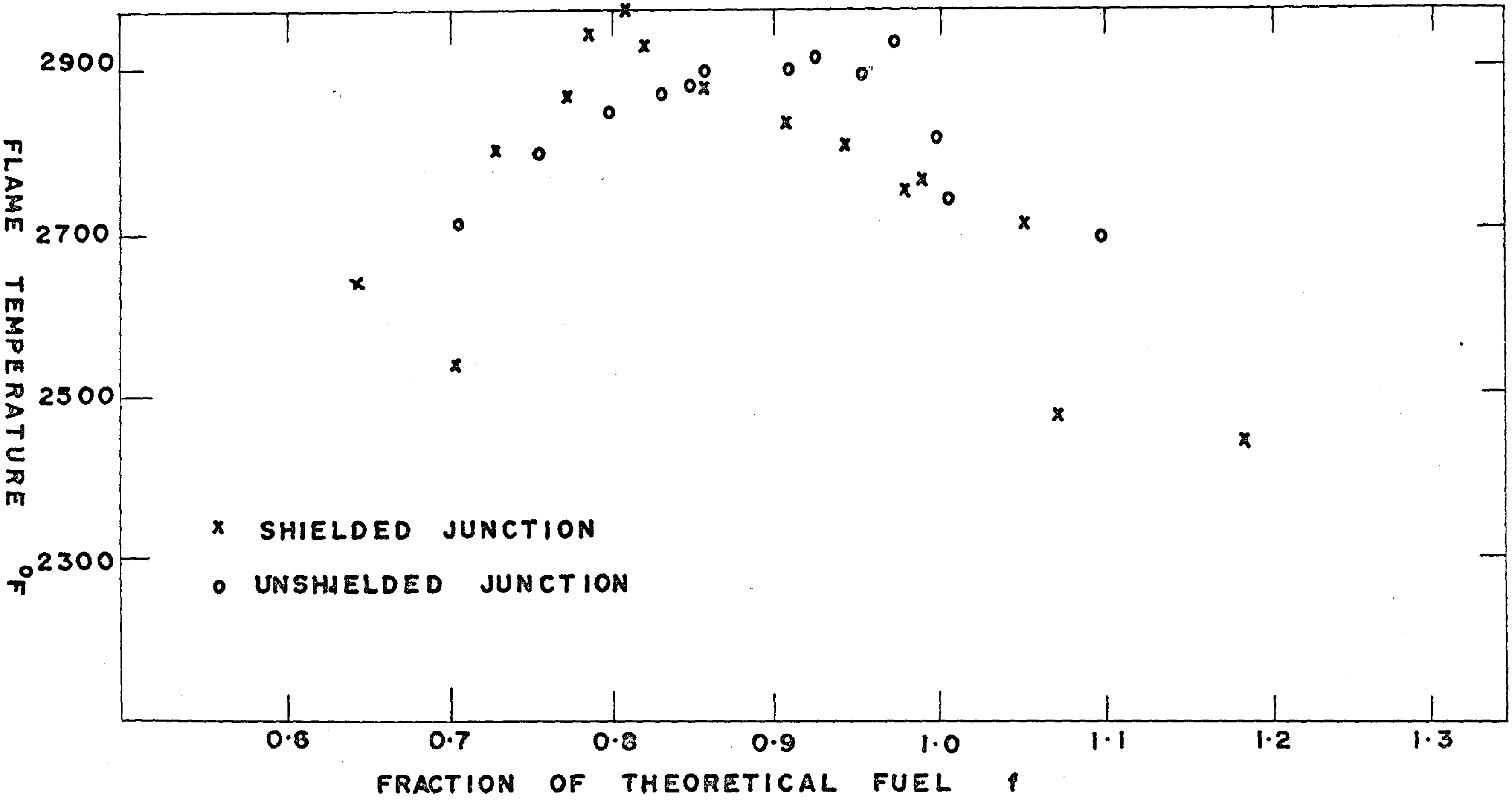

Fig. 24. Comparison of Flame Temperatures Measured with Shielded and Unshielded Thermocouple Junction

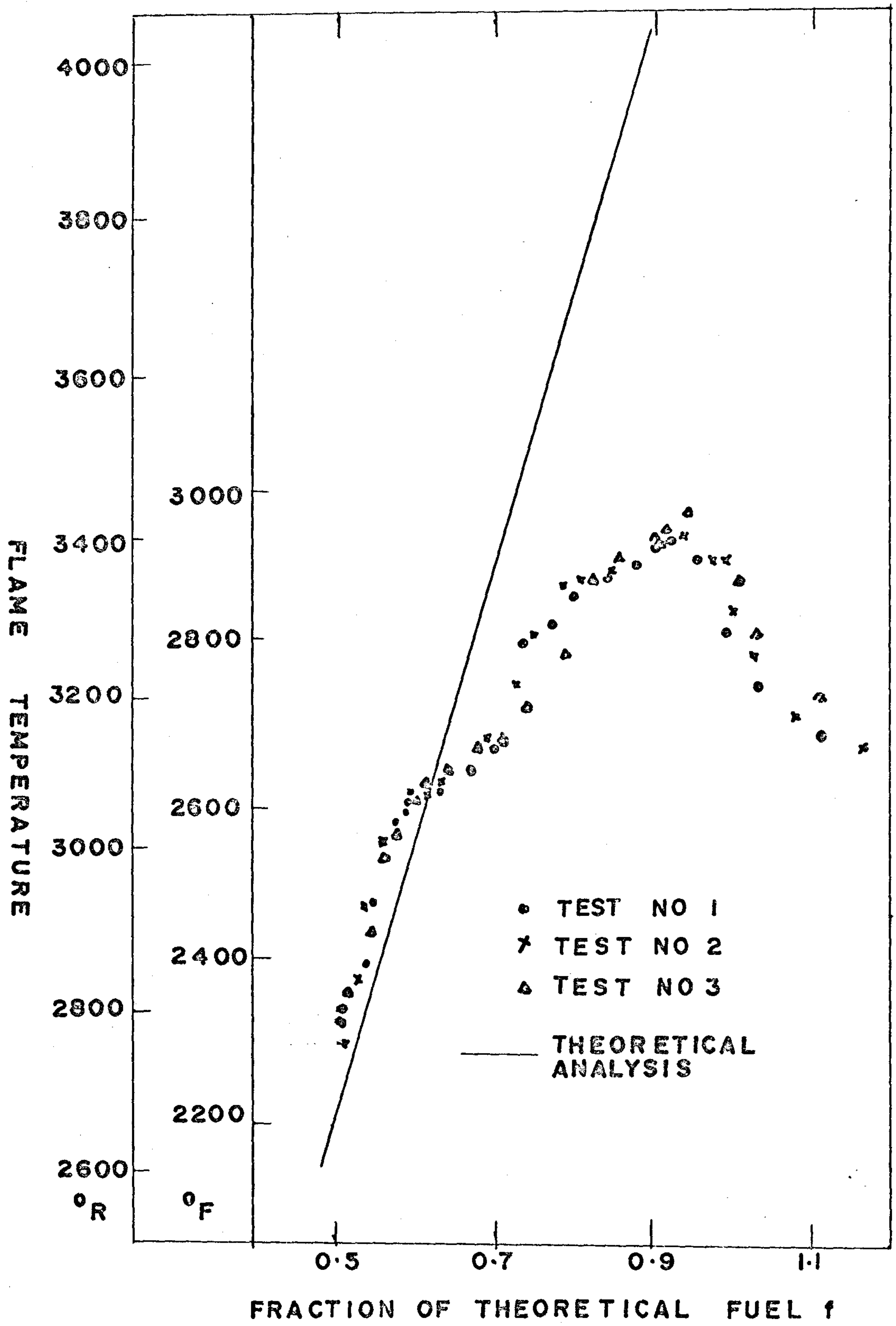

Fig. 25. Experimental and Theoretical Flame Temperatures vs Fraction of Theoretical Fuel

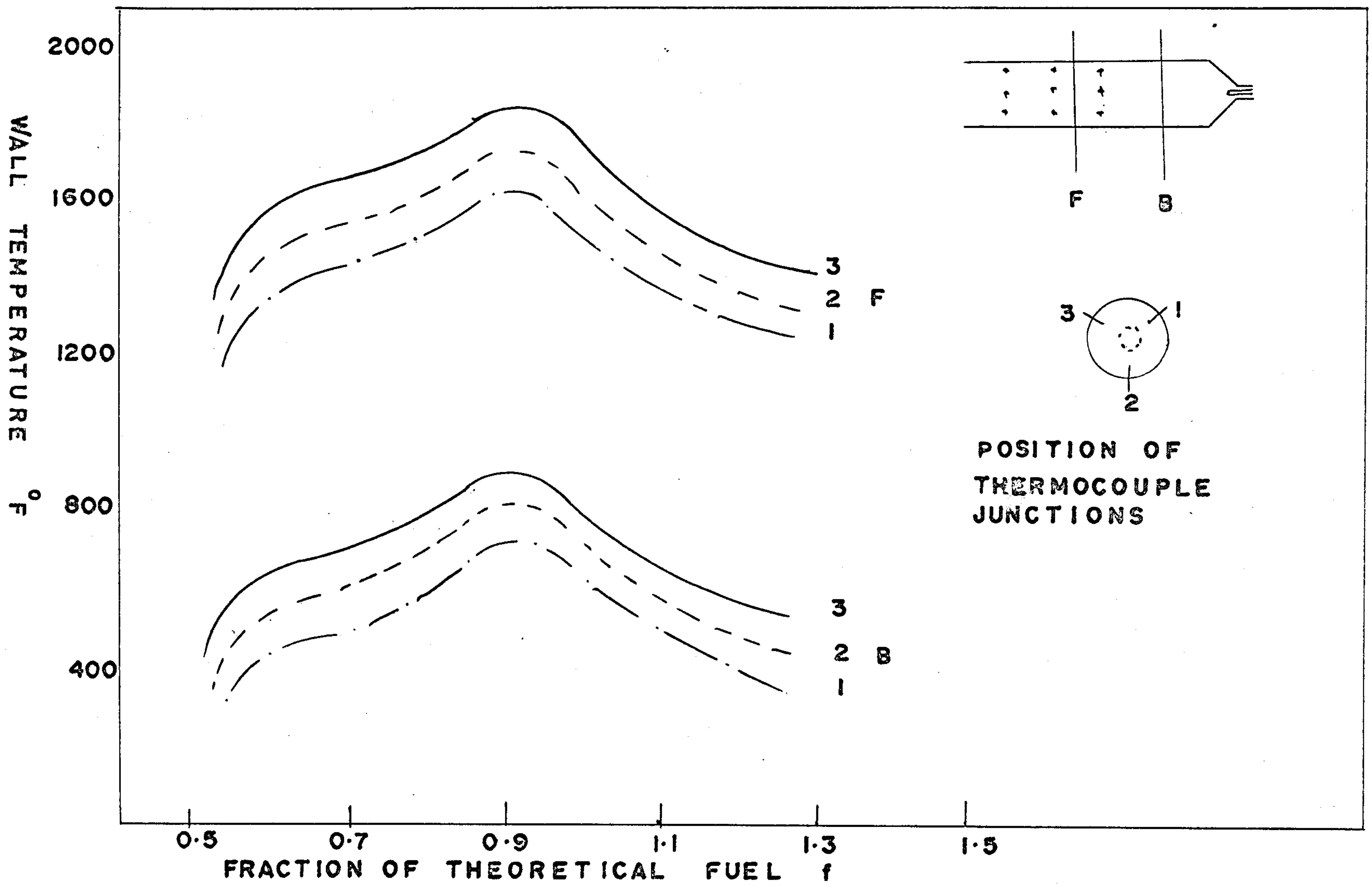

Fig. 26. Flame Tube Wall Temperatures vs Fraction of Theoretical Fuel

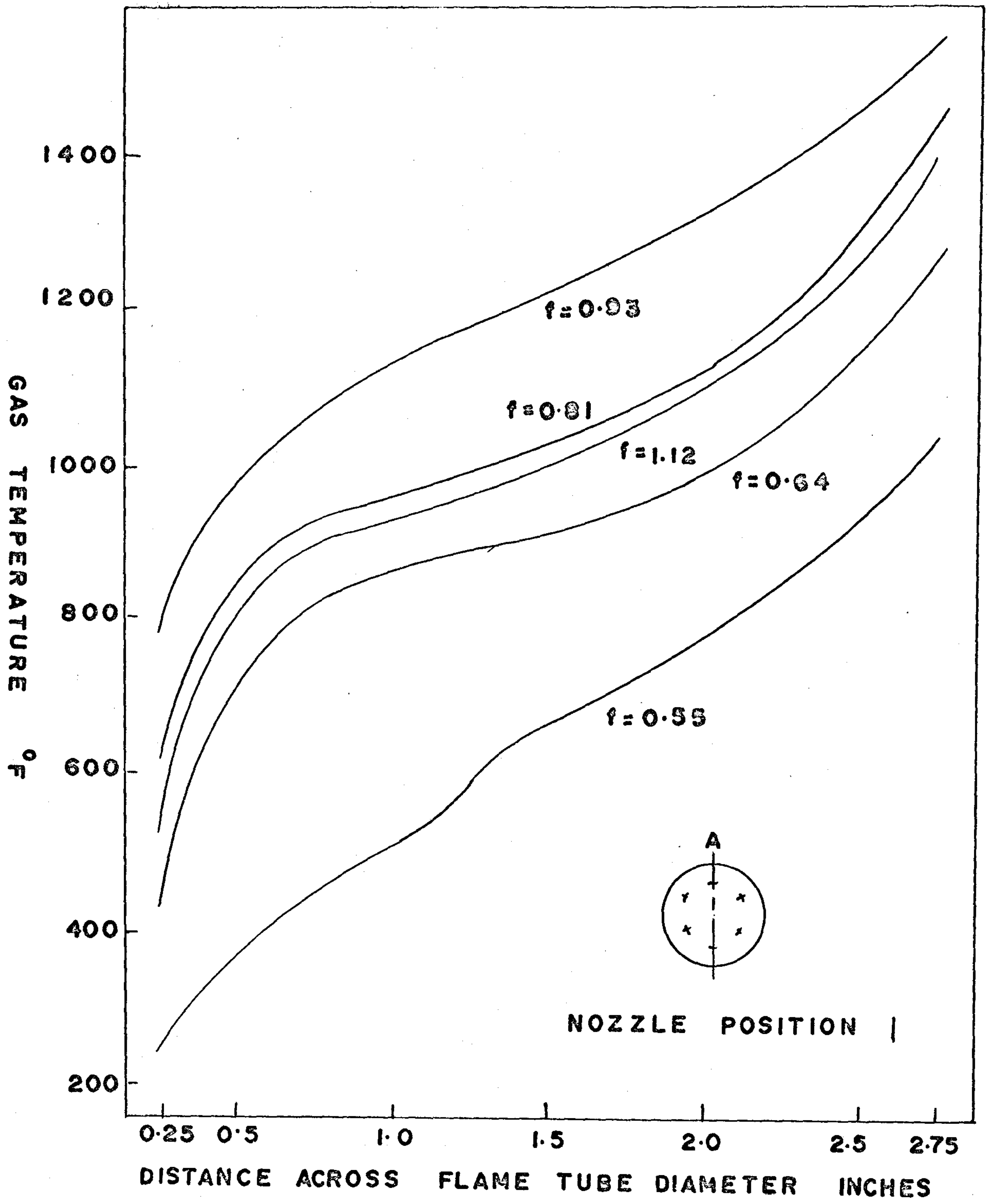

Fig. 27. Flame Tube Exit Plane Gas Temperature

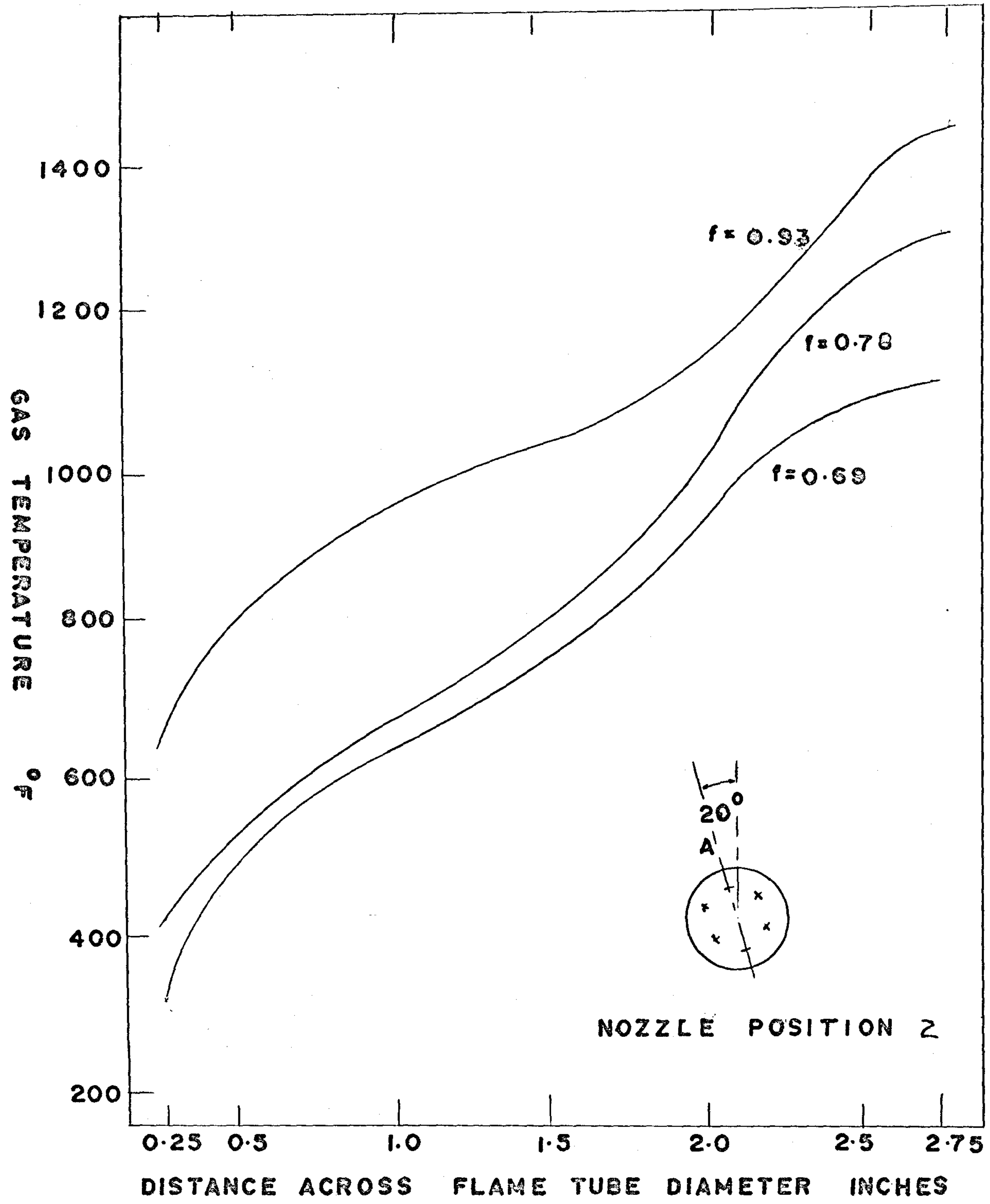

Fig. 28. Flame Tube Exit Plane Gas Temperature

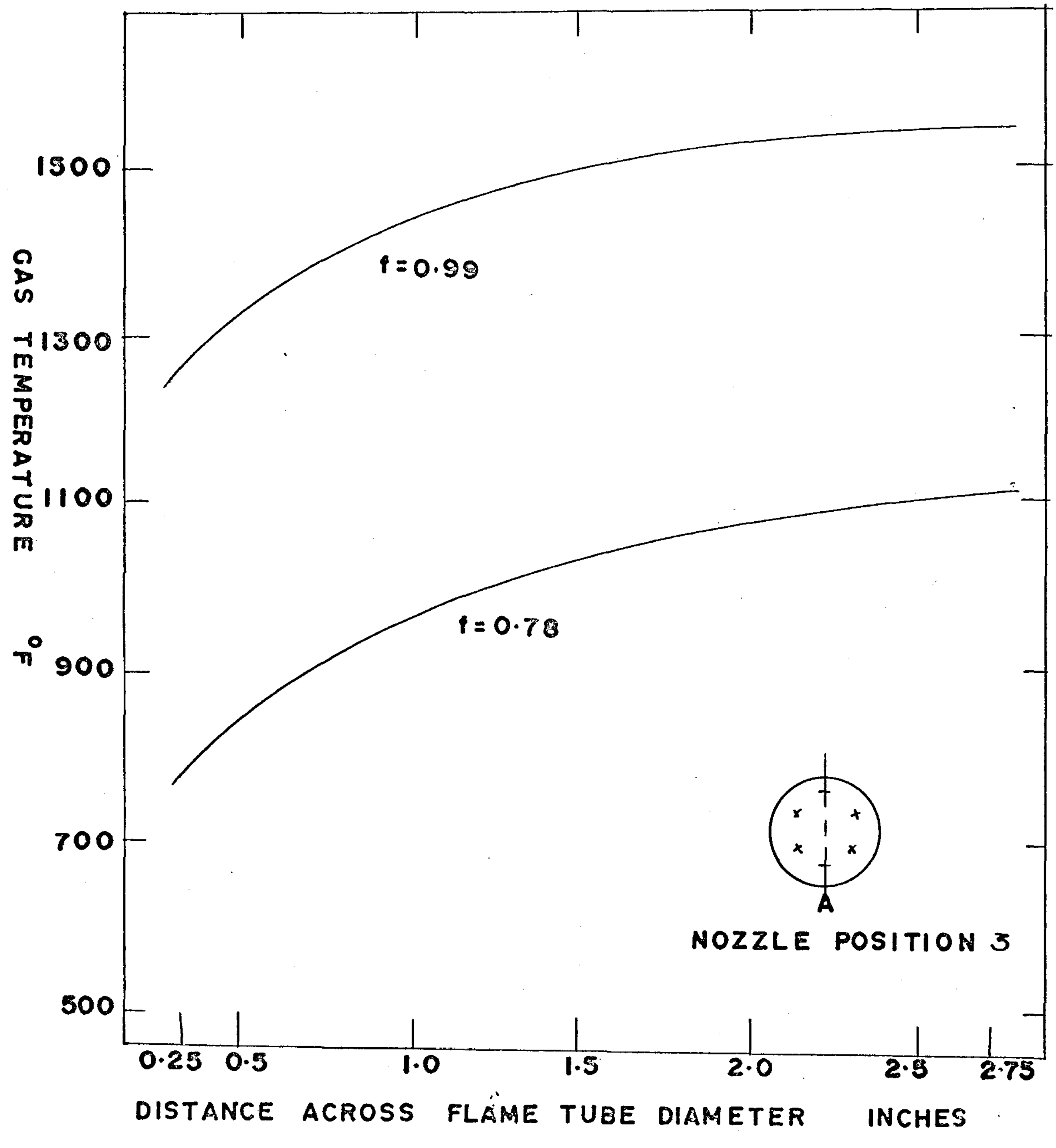

Fig. 29. Flame Tube Exit Plane Gas Temperature

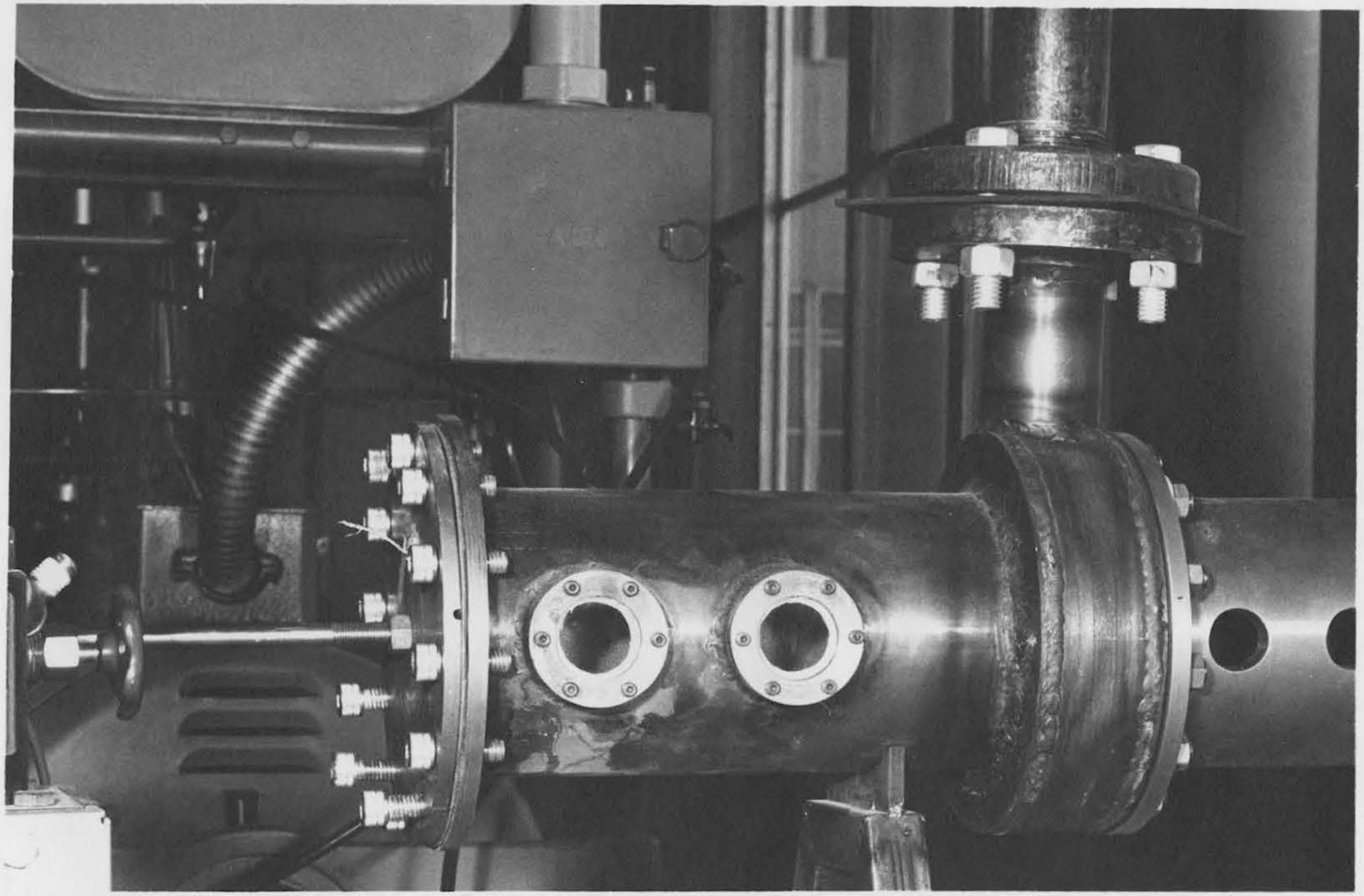

Fig. 30. Combustion Chamber Assembly

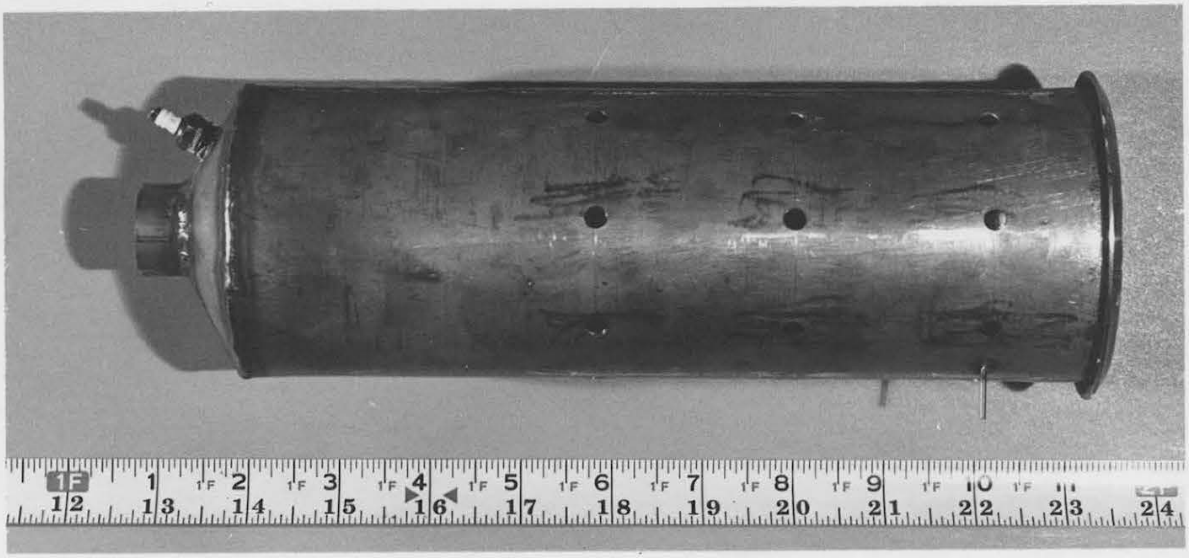

Fig. 31. The Flame Tube

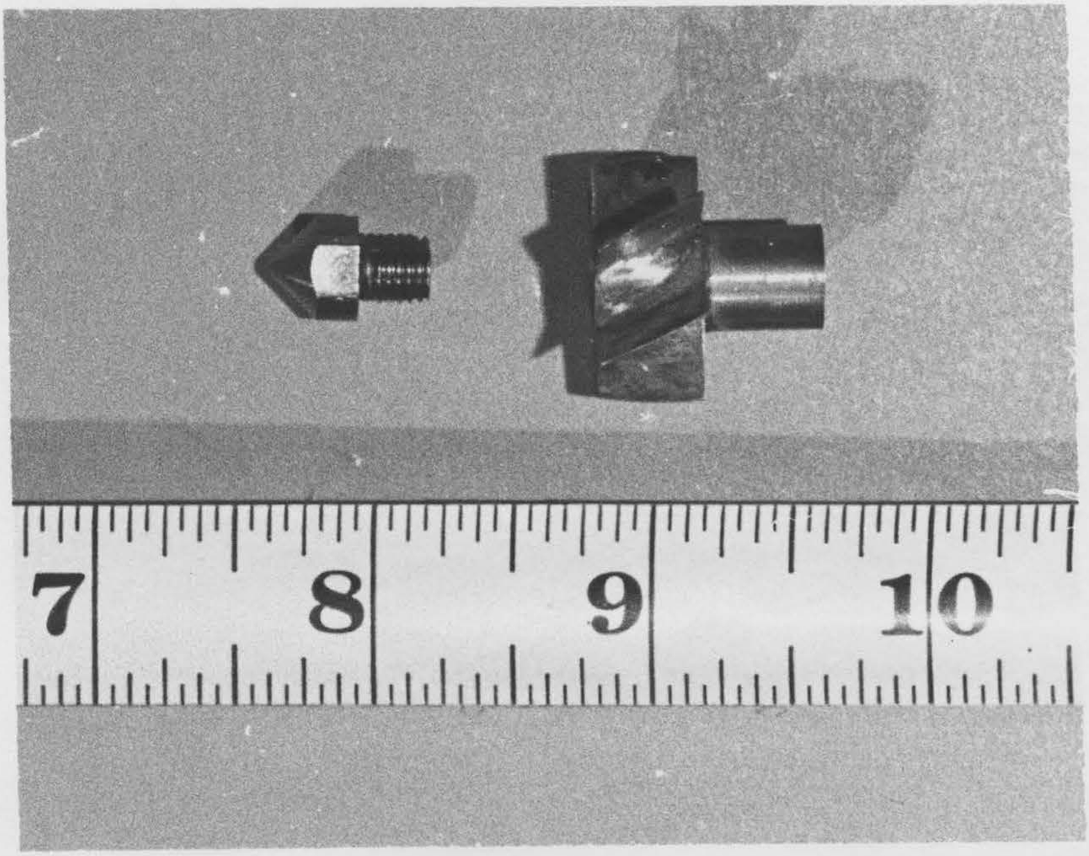

Fig. 32. The Gas Nozzle and Air Swirler

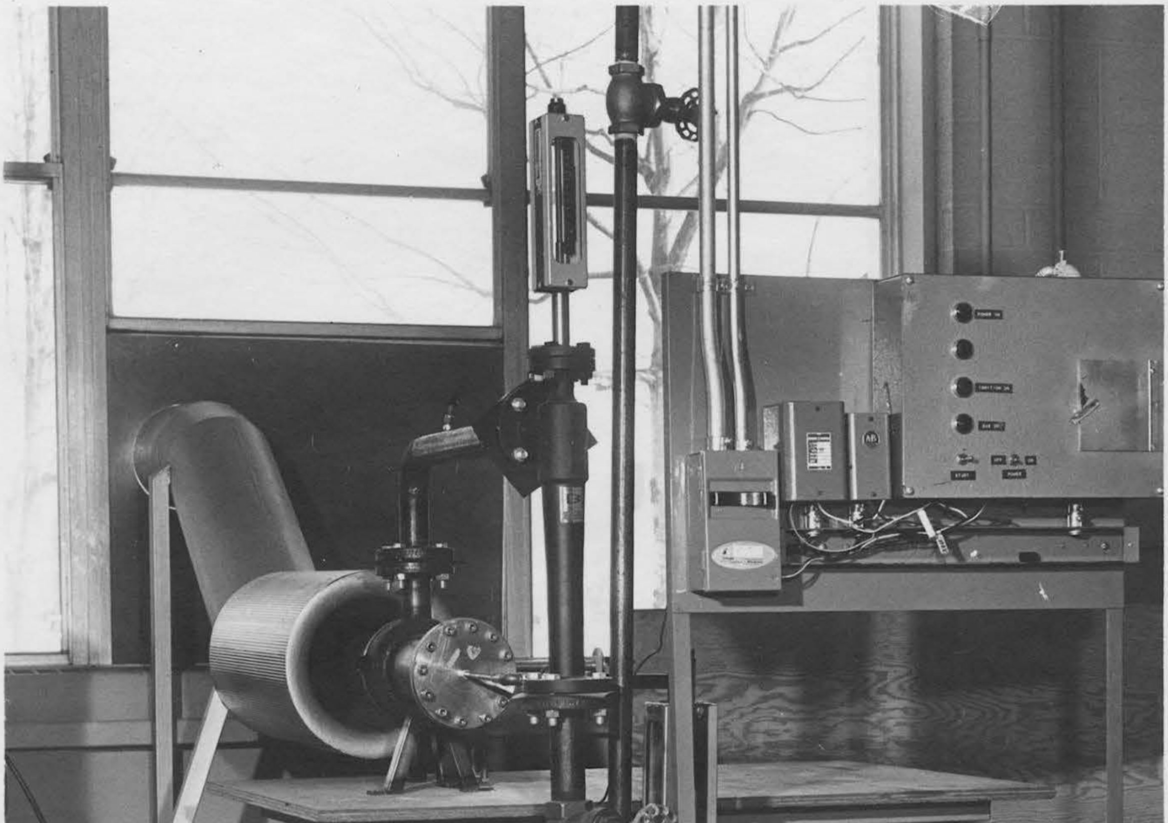

Fig. 33. View of Test Facility

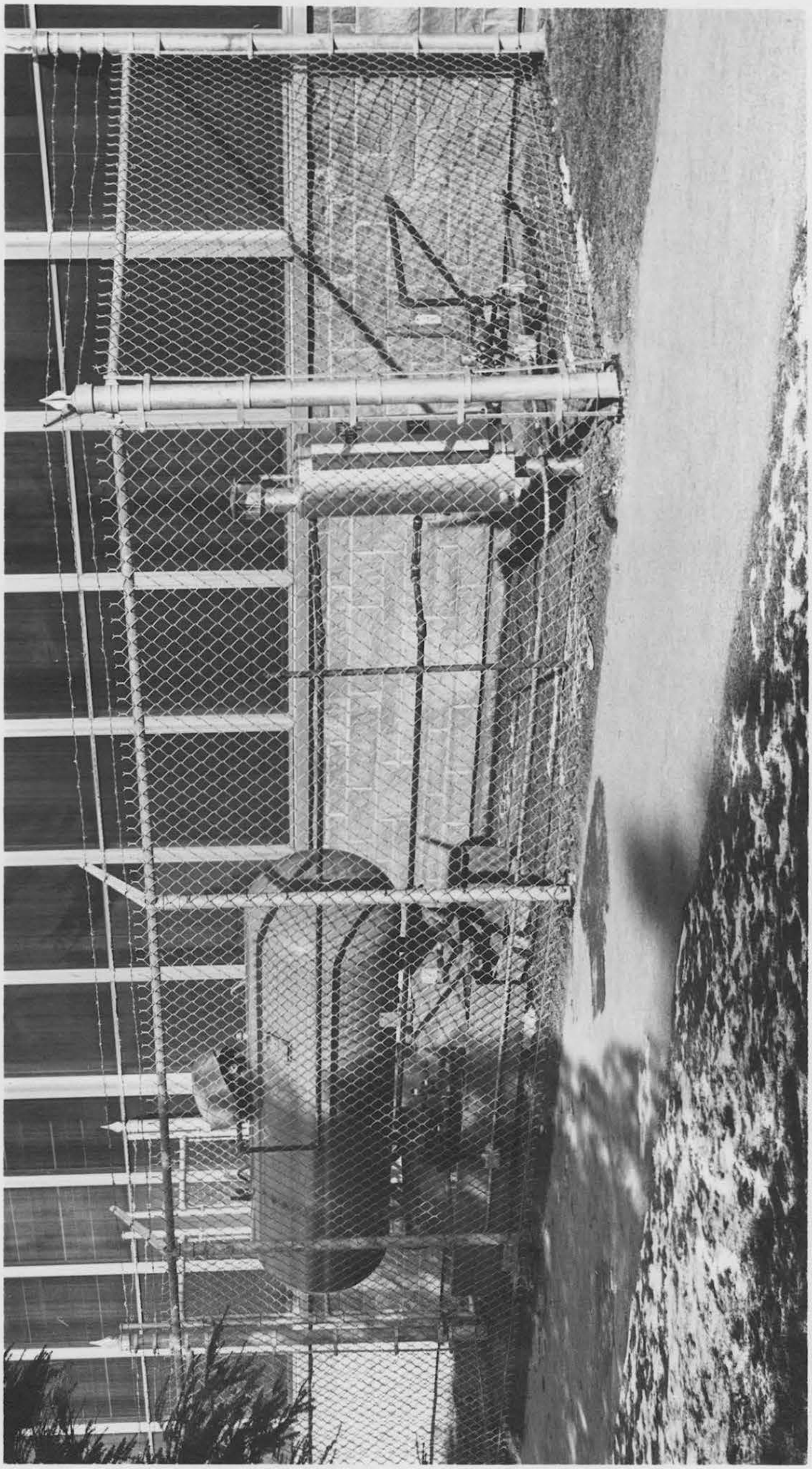

Fig. 34. Propane Tank and Vaporiser

Fig. 35. Gas Vaporiser and Supply Line To The Combustion Chamber

II. APPENDIX

II.1 Properties of Hastelloy Alloy X

A. Hastelloy Alloy X is the trade mark of the hot temperature alloy made by Union Carbide Canada Limited.

B. Typical Uses:

Has exceptional strength and oxidation resistance up to 2200°F; is useful for many industrial furnace applications because of its resistance to oxidizing, neutral and carburizing atmospheres; has had wide use for aircraft parts. The upper limit of usefulness is just above 2200°F.

C. Density at 72°F. 8.23 g. per cu. cm. (0.297 lb. per cu. in.)

D. (i) Liquidus Temperature.

Approximately 2350°F

(ii) Thermal Expansion, micro-in/in/°C.

79 to 212°F 13.8

79 to 1800°F 16.6

(iii) Specific Heat 0.105 cal/gm/°C

(iv) Thermal Conductivity at 60°F, 0.097 watt-cm/sq. cm/°C.

E. Colour, Silvery

F. General Resistance to Corrosion

This alloy is used mostly for its resistance to heat and oxidation, and only rarely to resist attack from aqueous solutions at ordinary temperatures.

G. Annealing temperature. 2150°F

H. Heat treatment. Solution treated at 2150°F, followed by either a rapid air cool or water quench. This ensures maximum ductility, corrosion resistance and machinability.

I. Composition of Sample Used.

Nickel 48.893%, Chromium 21.02%, Tungsten 0.50%, Iron 17.67%, Carbon 0.07%, Silicon 0.76%, Cobalt 1.44%, Manganese 0.55%, Molybdenum 9.08%, Phosphorus 0.015%, Sulpher 0.003%.

J. Mechanical Properties at Room Temperature

The Ultimate Tensile Strength is 111,900 p.s.i.; the 0.2% Yield Strength is 49550 p.s.i. and the percent Elongation on 2 inches is 45%.

This information was taken from Metals Handbook, Vol. 1, 8th Ed., American Society for Metals, 1961.

11.2

TABULATED RESULTS

1. FLAME TEMPERATURE WITH UNSHIELDED THERMOCOUPLE

T = FLAME TEMPERATURE °F

f = FRACTION OF THEORETICAL FUEL

TEST NO. 1		2		3	
f	T	f	T	f	T
0.52	2354	0.51	2303	0.52	2341
0.54	2402	0.53	2387	0.53	2368
0.55	2478	0.55	2472	0.56	2441
0.57	2560	0.57	2558	0.57	2536
0.58	2583	0.57	2576	0.58	2563
0.59	2592	0.59	2598	0.59	2581
0.6	2608	0.6	2612	0.6	2604
0.62	2615	0.62	26.7	0.63	2624
0.64	2620	0.64	2623	0.65	2647
0.67	2641	0.68	2653	0.67	2655
0.7	2675	0.71	2681	0.69	2672
0.74	2810	0.73	2753	0.71	2687
0.77	2842	0.76	2812	0.75	2724
0.81	2860	0.79	2841	0.8	2794
0.84	2889	0.82	2871	0.83	2876
0.88	2906	0.85	2892	0.87	2912
0.91	2924	0.87	2917	0.91	2937
0.93	2933	0.92	2931	0.93	2945
0.96	2904	0.94	2947	0.95	2968
0.99	2865	0.98	2902	0.98	2912
1.01	2812	1.01	2845	1.02	2884
1.04	2751	1.03	2790	1.04	2815
1.12	2689	1.09	2712	1.11	2733
1.18	2632	1.17	2671	1.18	2692
1.22	2584	1.21	2602	1.21	2605
1.27	2472	1.26	2498	1.27	2527
1.34	2339	1.32	2373	1.34	2412
1.48	2229	1.45	2285	1.47	2297
1.65	2074	1.62	2142	1.64	2123
1.88	1991	1.85	2037	1.87	2018
1.92	1963	1.91	1971	1.93	1971
2.06	1892	2.08	1917	2.05	1942

2. FLAME TUBE WALL TEMPERATURE WITH THE GAS NOZZLE IN POSITION 1

f	T_{1F}	T_{2F}	T_{3F}	T_{1B}	T_{2B}	T_{3B}
0.52	1174	1263	1347	301	362	422
0.54	1207	1298	1375	315	398	445
0.55	1272	1373	1447	347	453	562
0.58	1363	1467	1568	404	556	640
0.62	1393	1501	1597	448	572	668
0.7	1421	1537	1633	489	613	692
0.74	485	1562	1684	539	662	743
0.84	1571	1677	1763	633	751	845
0.93	1657	1762	1852	727	847	936
1.04	1415	1512	1626	542	633	714
1.27	1262	1371	1451	353	448	553

3. EXIT PLANE TEMPERATURE

3.1 NOZZLE POSITION 1

X = DISTANCE FROM ONE WALL OF FLAME TUBE

X inches	1/4	1/2	1	1-1/2	2	2-1/2	2-3/4
f	TEMPERATURE °F						
0.55	259	369	493	629	732	920	994
0.58	277	501	679	840	872	1076	1127
0.6	305	592	742	852	884	1094	1214
0.62	378	661	784	866	896	1105	1232
0.64	431	693	829	888	927	1136	1237
0.67	464	722	841	892	941	1155	1262
0.7	492	747	876	903	972	1188	1293
0.74	536	788	892	927	1003	1204	1342
0.78	577	822	905	951	1042	1258	1401
0.81	613	827	922	985	1077	1284	1423
0.84	642	861	942	1003	1104	1301	1450
0.86	687	887	982	1061	1162	1335	1471
0.91	732	938	1041	1135	1241	1372	1503
0.93	781	972	1104	1232	1329	1406	1522
0.96	763	947	1052	1204	1301	1381	1501
0.99	662	898	1036	1132	1242	1359	1479
1.01	604	867	976	1087	1194	1305	1452
1.04	573	834	923	1023	1153	1277	1401
1.12	542	801	876	922	1092	1264	1382

3.2. NOZZLE POSITION 2

X inches	1/4	1/2	1	1-1/2	2	2-1/2	2-3/4
f	TEMPERATURE °F						
0.69	314	495	672	794	948	1111	1153
0.73	336	503	687	801	988	1155	1199
0.78	418	513	703	821	1031	1249	1304
0.86	432	537	761	908	1078	1287	1352
0.93	604	838	966	1033	1180	1389	1464
1.09	784	925	1051	1148	1304	1520	1585

3.3 NOZZLE POSITION 3

X inches	1/4	1/2	1	1-1/2	2	2-1/2	2-3/4
f	TEMPERATURE °F						
.78	782	877	954	1021	1056	1131	1157
.82	858	932	1019	1076	1111	1181	1191
1.09	1249	1360	1444	1470	1510	1520	1551

4. FLAME TEMPERATURE

T_1 = FLAME TEMPERATURE USING SHIELDED THERMOCOUPLE

T_2 = FLAME TEMPERATURE USING UNSHIELDED THERMOCOUPLE

f	T_1 °F	f	T_2 °F
0.75	2780	0.72	2511
0.8	2865	0.73	2698
0.83	2864	0.77	2836
0.85	2883	0.81	2944
0.92	2891	0.82	2921
0.93	2880	0.86	2883
0.96	2893	0.94	2808
0.97	2913	0.97	2766
1.0	2823	1.1	2727
1.01	2756	1.10	2458
1.1	2694		

11.3 Viscosity of Combustion Gas Mixture

In Section 3.D.5, the viscosity of the combustion gases was calculated by taking the proportional sum of the viscosities of the constituents. This is a close approximation to the value for the viscosity of a gas mixture of three components, by Buddenberg and Wilke (25), in the following equation

$$\mu_n = \sum_{i=1}^{3} \frac{x_i \mu_i}{1 + x_i \left(1 - \frac{1.385 \mu_i}{\rho_i D_i}\right)} \qquad (1)$$

where μ_n is the viscosity of the gas mixture

x_i is the mole fraction of a constituent gas

ρ_i is the density of a constituent gas at the temperature and total pressure of the mixture

D_i is the diffusion coefficient of a constituent gas into the mixture, and for three gases D_1 is given by

$$D_1 = \frac{1 - x_1}{\frac{x_2}{D_{12}} + \frac{x_3}{D_{13}}}$$

where D_{12} and D_{13} are the diffusion coefficients of gas 1 into gases 2 and 3 respectively, at the temperature of the gas mixture. A similar expression exists for D_2 and D_3. Arnold (26) gives the diffusion coefficient from gas 1 to gas 2 as

$$D_{12} = \frac{0.0322}{3600} \frac{T^{3/2}}{(V_1^{1/3} + V_2^{1/3})^2} \sqrt{\frac{1}{M_1} + \frac{1}{M_2}} \ \text{ft}^2/\text{sec} \qquad (2)$$

where T is the temperature in °K

V is the molecular volume of the gas at its boiling point in cc/gm mole

M is the molecular weight of the gas

We are considering carbon dioxide, nitrogen and water vapour, and using equation (2), we have

$$D_{CO_2} = 0.00434\ ft^2/sec$$

$$D_{N_2} = 0.005\ ft^2/sec$$

$$D_{H_2O} = 0.00595\ ft^2/sec$$

Hence

$$\left(\frac{D\rho}{\mu}\right)_{CO_2} = 1.98$$

$$\left(\frac{D\rho}{\mu}\right)_{N_2} = 1.33$$

$$\left(\frac{D\rho}{\mu}\right)_{H_2O} = 1.17$$

The term $x_i \left(1 - \frac{1.385\mu_i}{\rho_i D_i}\right)$ is calculated and for

CO_2 is equal to $+0.0346$

N_2 is equal to -0.0292

H_2O is equal to -0.0276

In all cases this term is very small compared with unity, and can therefore be ignored in equation (1). The viscosity of the gas mixture is then as described in Section 3.D.5.

REFERENCES

1. W. T. Trick, "An Experimental Study of a Jet Driven Compressible Vortex", Master of Engineering Thesis, McMaster University, May 1966.

2. R. J. Rosa, "Physical Principles of M.H.D. Power Generation", The Physics of Fluids, Vol. 4, No. 2, February 1961.

3. "Flames Seeded with Alkali Metal Compounds", M. S. Thesis, Mechanical Engineering, Northwestern University, Illinois, October 1961.

4. P. Sporn, A. Kantrowitz, "Magnetohydrodynamics-future Power Process?", Design and Equipment Application Section, Power, Nov. 1959.

5. W. S. Lewellen, W.R. Grabowsky, "Nuclear Space Power Systems Using Magnetohydrodynamic Vortices", American Rocket Society Journal, May 1962.

6. G. J. Mullaney, N. R. Dibelius, "Small M.H.D. Power Generator Using Combustion Gases as an Energy Source", ARS Journal, April 1961.

7. A.H. Lefebvre, M.V. Herbert, "Heat Transfer Processes in Gas Turbine Combustion Chambers", Proc. Institute of Mechanical Engineering, England 1957.

8. J.S. Clarke, "A Review of Some Combustion Problems Associated With the Aero Gas Turbine", Journal of the Royal Aeronautical Society, April 1956.

9. Unpublished Information from Orenda Ltd., Malton, Ontario.

10. C.V. Humble, W.H. Lowdermilk, L.E. Desmon, "Measurements of Average Heat Transfer Coefficients for Subsonic Flow of Air in Smooth Tubes at High Surface and Fluid Temperatures", NACA Report 1020, 1951.

11. W.H. McAdams, "Heat Transmission", Third Edition, McGraw Hill Book Company, New York, 1954.

12. S.R. Montgomery, K. Weiss, "Forced Convection Heat Transfer in Ducts of Non-Circular Cross Section", NEL Report I, National Engineering Laboratory, Glasgow, 1961.

13. R. L. Judd, J.H.T. Wade, "Forced Convection Heat Transfer in Eccentric Annular Passages", Proc. Heat Transfer and Fluid Mechanics Institute, 1963.

14. F. Kreith, Principles of Heat Transfer, 2nd Edition, International Textbook Company, 1965.

15. H.C. Hottel, "Radiative Transfer in Combustion Chambers", Journal of the Institute of Fuel, England, Vol. 34, June 1961.

16. J. Hilsenrath, Y. S. Touloukian,"The Viscosity, Thermal Conductivity and Prandtl Number of Air, O_2,N_2,H_2, CO, CO_2, H_2O, H_e and A, Transactions ASME, 1954.

17. M.A. Knight, R.B. Walker, "Component Pressure Losses in Combustion Chambers", ARC R and M 2987, Aeronautical Research Council, England 1957.

18. R. T. Dittrich, R.C. Graves, "Discharge Coefficients for Combustor Liner Air Entry Holes", NACA TN 3663.

19. W.R. Hawthorne, G.F.C. Rogers, B.Y. Zaczek, "Mixing of Gas Streams - The Penetration of a Jet of Cold Air into a Hot Stream", RAE Technical Note Eng. 271, England, 1944.

20. J.H. Childs, "Flame Stabilization", Chapter V, High Speed Aerodynamics and Jet Propulsion Vo. XI, Design and Performance of Gas Turbine Power Plants, OUP, London 1960.

21. J. W. Haddock, "Flame Blow Off Studies of Cylindrical Flame Holders in Channeled Flow", Report 3-24, Jet Propulsion Laboratory, Cal. Inst. Tech. 1951.

22. F. Schmidt, "The Internal Combustion Engine", Chapman and Hall, 1965.

23. G. J. Van Wylen, "Thermodynamics, John Wiley and Sons, Inc., New York, 1959.

24. Massachusetts Institute of Technology, Aerodynamic Measurements, Gas Turbine Laboratory, 1953, Eagle Enterprises, Boston, Mass.

25. J. W. Buddenberg and C. R. Wilke, "Calculation of Gas Mixture Viscosities", Industrial and Engineering Chemistry, Vol. 41, 1949.

26. J. H. Arnold, "Studies in Diffusion", Industrial and Engineering Chemistry, Vol. 22, 1930.